Load Security Region Determination with Second Order Cone Programming Relaxation

Mr. Pongsakorn Sukheeboon

A Thesis Submitted in Partial Fulfillment of the Requirements

for the Degree of Master of Engineering in Electrical Engineering

Department of Electrical Engineering

FACULTY OF ENGINEERING

Chulalongkorn University

Academic Year 2020

การกำหนดพื้นที่ความปลอดภัยของโหลดด้วยการผ่อนคลายแบบการโปรแกรมกรวยอันดับสอง

นายพงศกร สุขีบุญ

Thesis Title   Load Security Region Determination with Second Order
                         Cone Programming Relaxation
By   Mr. Pongsakorn Sukheeboon
Field of Study   Electrical Engineering
Thesis Advisor   Associate Professor SOTDHIPONG PHICHAISAWAT, Ph.D.

Accepted by the FACULTY OF ENGINEERING, Chulalongkorn University in Partial Fulfillment of the Requirement for the Master of Engineering

.... Dean of the FACULTY OF
                                               ENGINEERING
(Professor SUPOT TEACHAVORASINSKUN, Ph.D.)

THESIS COMMITTEE

.... Chairman
(Associate Professor SURACHAI CHAITUSANEY, Ph.D.)

.... Thesis Advisor
(Associate Professor SOTDHIPONG PHICHAISAWAT, Ph.D.)

.... Examiner
(Assistant Professor Channarong Banmonkol, Ph.D.)

.... External Examiner
(Att Phayomhom, Ph.D.)

พงศกร สุขีบุญ : การกำหนดพื้นที่ความปลอดภัยของโหลดด้วยการผ่อนคลายแบบการ
โปรแกรมกรวยอันดับสอง. (Load Security Region Determination with Second
Order Cone Programming Relaxation) อ.ที่ปรึกษาหลัก : รศ. ดร.โสตถิพงศ์ พิชัย
สวัสดิ์

ความต้องการไฟฟ้าสูงสุดของประเทศไทยเพิ่มขึ้นอย่างต่อเนื่อง เมื่อความต้องการโหลด
เพิ่มขึ้นการผลิตไฟฟ้าจะเพิ่มขึ้นเพื่อตอบสนองต่อโหลด อย่างไรก็ตามความต้องการโหลดไม่
สามารถเพิ่มขึ้นเกินกว่าข้อจำกัดของระบบไฟฟ้าซึ่งรวมถึง ขีดจำกัดขนาดแรงดัน ขีดจำกัดเครื่อง
กำเนิดไฟฟ้า และขีดจำกัดของสายส่ง งานวิจัยนี้กำหนดขอบเขตความปลอดภัยของโหลดซึ่งเป็น
พื้นที่ที่เป็นไปได้ของระบบไฟฟ้า พื้นที่ความปลอดภัยของโหลดคือชุดของคำตอบของระบบไฟฟ้าซึ่ง
ไม่ละเมิดข้อจำกัดของระบบไฟฟ้า ขอบเขตความปลอดภัยของโหลดจะพิจารณาโดยใช้อัลกอริทึม
การติดตาม วิธีนี้ประกอบด้วยกระบวนการทำนายและกระบวนการแก้ไข กระบวนการแก้ไขเป็น
วิธีการเพิ่มประสิทธิภาพที่ใช้เพื่อค้นหาเส้นทางที่สั้นที่สุดระหว่างจุดทำนายและจุดขอบเขต ยิ่งไป
กว่านั้นงานวิจัยนี้ได้กำหนดวิธีการเพิ่มประสิทธิภาพ ซึ่งเป็นแบบไม่เชิงเส้นและไม่คอนเวกซ์ ให้
กลายเป็นปัญหาคอนเวกซ์ โดยใช้การผ่อนคลายแบบการโปรแกรมกรวยอันดับที่สอง ผลลัพธ์แสดง
พื้นที่ความปลอดภัยของโหลดของระบบไฟฟ้าทดสอบ ขอบเขตความปลอดภัยของโหลดจะแสดงใน
ระนาบ P-Q ขอบเขตนี้สามารถใช้เพื่อกำหนดจุดปฏิบัติการของระบบไฟฟ้าซึ่งไม่ละเมิดข้อจำกัด
ของระบบไฟฟ้า นอกจากนี้ยังสามารถใช้พื้นที่ความปลอดภัยของโหลดเพื่อวางแผนการทำงานของ
ระบบไฟฟ้าเช่นการปลดโหลดและการติดตั้งเซลล์แสงอาทิตย์ พื้นที่ความปลอดภัยของโหลด
สามารถเพิ่มหรือเคลื่อนย้ายได้เนื่องจากพารามิเตอร์ระบบจากการดำเนินการที่ได้กล่าวมาข้างต้น
ดังนั้นการดำเนินการเหล่านี้สามารถเปลี่ยนรูปร่างขอบเขตความปลอดภัยของโหลดได้

สาขาวิชา	วิศวกรรมไฟฟ้า	ลายมือชื่อนิสิต ....
ปีการศึกษา	2563	ลายมือชื่อ อ.ที่ปรึกษาหลัก ....

6272055821 : MAJOR ELECTRICAL ENGINEERING

KEYWORD: Load security region, Tracing algorithm, Second-order cone programming relaxation, Alternating current optimal power flow, Continuation method

Pongsakorn Sukheeboon : Load Security Region Determination with Second Order Cone Programming Relaxation. Advisor: Assoc. Prof. SOTDHIPONG PHICHAISAWAT, Ph.D.

Thailand's electricity peak demand is increasing continuously. When load demand increases, power generation will increase to respond to the load. However, load demand cannot increase beyond power system constraints which include voltage magnitude limit, generation limit, and transmission line limit. This work determines the load security region which is the feasible region of the power system. The load security region is a set of power system solution which does not violate the power system constraints. The load security region is considered by using a tracing algorithm. This method consists of predictor process and corrector process. The corrector process is an optimization-based method that is used to find the shortest path between the prediction point and the boundary point. Moreover, this work formulates optimization-based method which is nonlinear and nonconvex to be convex by using second order cone programming (SOCP) relaxation. The results show that the load security region of the power system test case. The load security region is represented in the P-Q plane. In addition, the load security region can be used to plan the power system operation, such as load shedding, and photovoltaic (PV) installation. The load security region can be increased or moved due to the system parameter from these operations. Thereby, these operations can change the load security region shape.

Field of Study:	Electrical Engineering	Student's Signature	....
Academic Year:	2020	Advisor's Signature	....

ACKNOWLEDGEMENTS

TABLE OF CONTENTS

LIST OF TABLES

Page

LIST OF FIGURES

CHAPTER 1

Introduction

1.1 Background and Motivation

Nowadays, load peak demand is increasing every year for each power system. Power transfer is the key factor of the power system analysis. Thus, power system operation becomes more important as the load demand increases. When the load demand increases rapidly, the generator must also increase production capacity. Then, the power system will operate near the critical point [1] because of power system limit, such as voltage magnitude, generation limit, transmission line limit, and others. The operating point must satisfy power system constraints. On the other words, the power system operation must supply power to the consumers without the violation. Load determination is applied to this problem to determine load increasing for the reliability and security.

Load determination can be obtained by several conventional method [2]. For example, repeated power flow (RPF), continuous power flow (CPF), and optimization method. Load determination is used to obtain the maximum loading point. This point is an operating point which do not exceed the power system constraints. This work applies tracing algorithm to obtain the load determination. Tracing algorithm bases on continuation method [3] which comprises 2 processes. The first process is predictor process and the other is corrector process. Moreover, tracing algorithm includes the initial guess and first prediction point.

Conventional corrector process is the vector operation. Consequently, this process is replaced by optimization-based method in [4]. Additionally, the optimization-based method consists of 2 parts. The first part is objective function. The objective function is used to find the shortest path between the prediction point which is outside the feasible region and the power flow solution point on the boundary. The second part is power system constraints. This part is used to limit the power system variables.

The solution point is called correction point. However, the optimization-based method is the optimal power flow (OPF) problem which is nonlinear and nonconvex problem. Furthermore, the OPF problem is NP-hard and challenging problem. This research proposes second order cone program (SOCP) relaxation in [5] to convexify the classic optimization as convex format. As a result, the classic optimization problem is replaced by SOCP relaxation. Besides, tracing algorithm with SOCP relaxation is used to determine the load security region.

The shape of the load security region is changed due to the effects of system parameters in [6]. SOCP relaxation can be applied with the additional devices, for instance, distributed generation (DG) installation in [7], system parameter changing and other devices which supplies or consumes the power from the system in [8]. The original load security region cannot satisfy the power system constraints with the new parameters because the power flow equations are not the same as the previous equations. Thereby, the original load security region is reshaped into a new load security region according to the effects of system parameters.

The purpose of this thesis is to formulate classic optimization problem as convex format by SOCP relaxation and visualize the load security region of power system by using tracing algorithm with SOCP relaxation. Moreover, the load security region must be power flow solution set where the solutions do not violate the power system limit.

1.2 Objective

1. To determine load security region by using tracing algorithm.

2. To develop the optimization-based method of tracing algorithm by using second order cone programming relaxation.

3. To analyze the effects of system parameters to visualize load security region.

1.3 Scope of Works

1. This work determines only the power system which operates in a steady state.

2. This work defines the power system constraints as following

   2.1 Bus voltage limits,

   2.2 Generator limits, and

   2.3 Branch flow limits.

3. This work considers only SOCP relaxation of the convex optimization problem.

4. The power system parameters are obtained from MATPOWER cases.

5. This work considers 2 source-sink pair as following

   5.1 generator buses to load bus,

   5.2 area to area.

6. This work focuses only the effects of solar cell and load shedding.

1.4 Methodology

1. Studying literature works related to the load security region determination.

2. Studying literature works related to optimization-based method by SOCP relaxation.

3. Studying CVX which is an optimization solver and MATLAB.

4. Formulating the optimization-based method from conventional method which is non-convex problem to convex problem by using second order cone program relaxation.

5. Studying the effects of system parameters to the load security region.

6. Visualizing the load security region of the proposed method on test systems.

7. Discussing the result and concluding the study.

1.5 Expected Contribution

1. Load security region.

2. Obtaining the solution of the power system within the security limit.

3. Load security region variation.

1.6 Literature Review

Nowadays, load peak demand increases due to urbanization. Load security region is the key factor to determine the operating point of power system. The load security region is a feasible region of the power flow solution which do not violate the power system constrains. The literature review of this work consists of 2 sections. The first section is the development of tracing algorithm. The second section is the development of optimization problem with SOCP relaxation.

To determine load increasing, there are serval methods, e.g., RPF in [2], CPF in [1], and optimization method in [2]. RPF is to determine load margin by increasing the load via power flow analysis when the load demand increase, the generator increases the power generation. This process will be repeated until the power system collapses. CPF is like RPF. This method is used to consider load margin from the relation of voltage stability and load demand. When the load demand increases, the voltage will response to the load change until the power system collapses. Optimization method is to find the maximum load point from the optimization. All ablove methods can determine only single point of the maximum load point. In fact, the maximum load point is not only a single point, but also the set of maximum load point on the boundary of the load security region in the relation of active and reactive power. For the reason above, continuation method from [3] is proposed. This method is to determine the load security region by predictor-corrector process. In addition, the corrector process is replaced by the conventional optimization-based method in [4] which is nonlinear and nonconvex problem.

To develop optimization-based method, the conventional optimization which is nonlinear and nonconvex problem is considered. [9] shows that the alternating current optimal power flow (ACOPF) is NP-hard and used for finding a feasible solution. Several methods have been proposed to solve the ACOPF problem, such as, approximation methods in [10]-[12] which modify the power flow equation by network structure, non-linear optimization method in [13]-[15], heuristic methods in [16]-[17], and convexification approaches in [5]. To convexify ACOPF, [18] proposes a linearized-relaxed model to approximate and solve the ACOPF problem. Whereas [19] proposes a semidefinite program (SDP) relaxation method. The application of moment-based relaxation for the OPF solution is investigated in [20] and [21]. The research [22] and [23] obtain the solutions of nonconvex optimization by using SDP relaxation. Besides, [24]-[28] propose SOCP relaxation to solve the ACOPF. Additionally, [25] investigates the geometry of the feasible injection. This work shows that SDP and SOCP relaxation are exact when the angle separation of voltage phasors of line terminals is sufficiently small and there is no bound on reactive power bus. However, the second condition cannot be used in the real power system. [28] presents that SOCP relaxation is computationally more efficient than the SDP relaxation. SOCP relaxation in [26] is tight where the condition is no upper bound on the load bus. [27] also shows that the relaxation is exact with no upper bound on the voltage-magnitude buses and specific condition involving the network parameters. Last but not least, [28] improve [27] by introducing the conservative constraints on the upper bound for the voltage-magnitude buses. Finally, ACOPF with SOCP relaxation is formulated from [5] and [29] by including branch limits and shunt elements to improve [28].

From the research above, this work is considered using continuation method and optimization with SOCP relaxation to propose tracing algorithm for visualizing load security region in order to prove the exactness of SOCP relaxation in [30].

CHAPTER 2

Load Margin Determination

Load expansion in power system must concern the load margin. Load margin is used to consider for determining active and reactive power demand of the power system to not exceed the security limits of the system and satisfy all power flow condition, e.g., bus voltage limits, generator limits, and branch flow limits. The load margin can be determined by many traditional methods. This chapter reviews power flow problem, load margin determination in [1] which consists of repeated power flow (RPF), continuation power flow (CPF), optimization method and classification of security region for load margin.

2.1 Power Flow Problem

The fundamental problem of the power system is the power flow analysis. The power flow equations are used to calculate power system variable for determining the appropriate operating point. The power flow variables consist of 4 sets of bus parameter which are the active power (P), the reactive power (Q), the bus voltage (U), and the voltage angle (δ). The power flow equations in [4] are shown as follow.

$$f - S = 0 \tag{2.1}$$

$$f = U \times (Y_{bus} \times U)^H, \tag{2.2}$$

$$U = U_m \times (\cos(\delta) + j\sin(\delta)), \tag{2.3}$$

where S is a vector of injection of active and reactive power to each bus. f is also the injection of active and reactive power to each bus calculated from equation (2). U is a vector of bus voltage and U is defined by equation (3). Y_{bus} is defined as nodal admittance matrix of the power system. The power flow equations of the power system are N equations where N is total bus number. Let a^H denote the conjugate form of a. Let j denote the imaginary unit.

2.2 Load Margin Determination

Load margin determination is used to obtain the maximum load of the power system. There are many methods to determine load margin, for example, repeat power flow (RPF), continuous power flow (CPF) and optimization method.

2.2.1 Repeated Power Flow

Repeated power flow in [2] is determined by lightly incremental power demand at the sink and the incremental power from the sources. Then, this method calculates the power flow equations repeatedly until the power system reaches limitation. The exceed limitation point is an unsolvable point. This method is used to balance the increased demand and losses in the system. Load demand increment is shown as follow.

$$P_{di,new} = P_{di,old} + k \tag{2.4}$$

$$Q_{di,new} = (P_{di,old} + k)\tan(\cos^{-1}(pf_i)) \tag{2.5}$$

Where

k is the load incremental step size.

$P_{di,new}$ is increased active power demand at bus i.

$P_{di,old}$ is previous active power demand at bus i.

$Q_{di,new}$ is increased reactive power demand at bus i.

pf_i is power factor of load changing at bus i.

2.2.2 Continuation Power Flow

Continuous power flow in [1] is used to obtain maximum load margin via the voltage collapse point of the power system. The voltage collapse and power system collapse may occur because power system cannot respond to every load increment due to power system conditions and events. Bifurcation theory is used to consider the change in the power system. Voltage collapse point is determined by parameter values

that bring about saddle-node bifurcations. Bifurcation characteristic is presented in equation (2.6).

$$F(x, \lambda) = \lambda - x^2 \tag{2.6}$$

Where

x is the state variable.

λ is a parameter.

The equilibrium point is x_0 and λ_0 where $F(x_0, \lambda_0) = 0$. The consideration of λ is divided into 3 conditions. First condition is $\lambda = 0$. This condition is only one point which is a saddle node point. Second condition is $\lambda < 0$. This condition is no equilibrium. Last condition is $\lambda > 0$. This condition has equilibrium points which are stable and unstable points as shown in Figure 2.1.
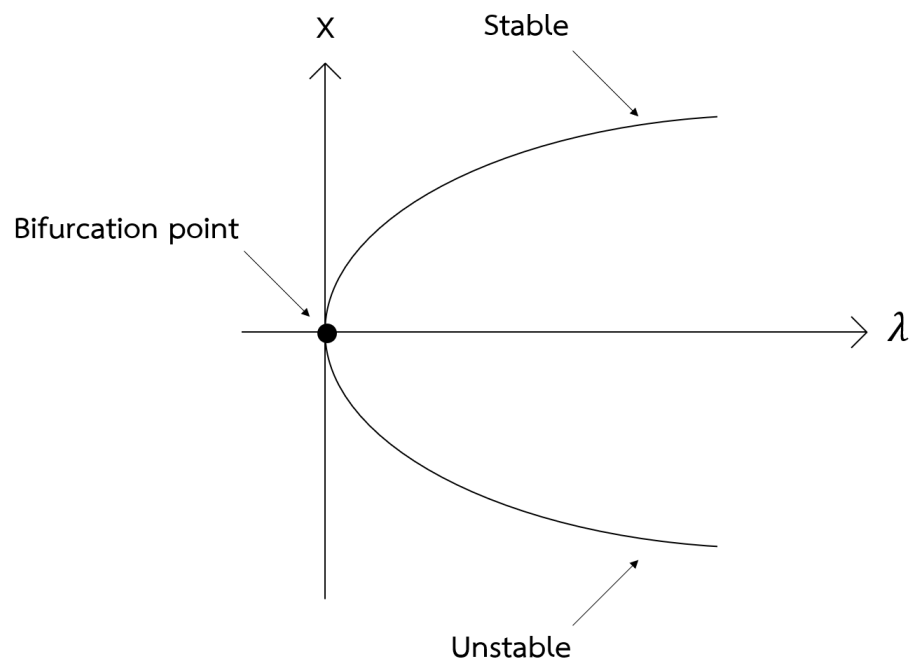
Figure 2.1 Bifurcation diagram

The power system problems are formulated with the Jacobean matrix for solving the problems. Jacobean matrix becomes singular when the power system limit and voltage stability reaches the limit. Continuation power flow is used to determine the critical point by using predictor and corrector scheme as shown in Figure 2.2. The

solution of this method is presented as the curve of power flow solutions. Y-axis is defined as bus voltage and X-axis is defined as load parameter. The critical point in the curve of power flow solutions is a maximum loading point.
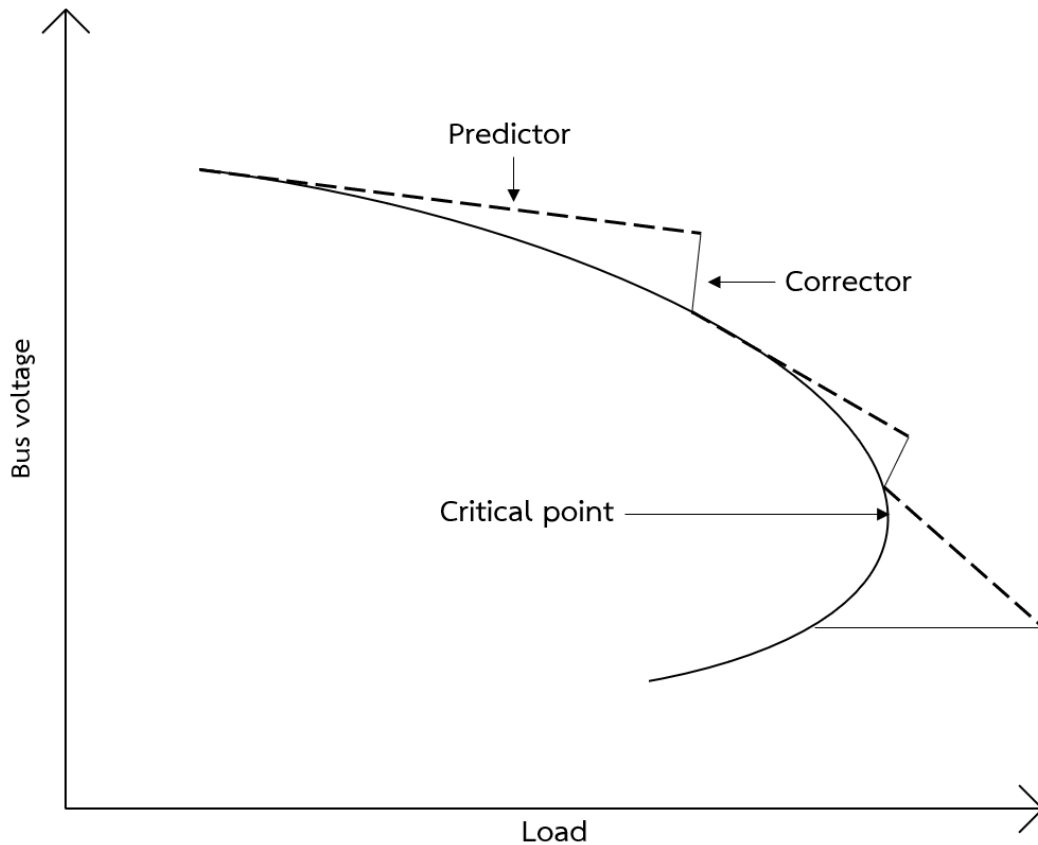
Figure 2.2 The predictor – corrector scheme

Power flow equations is presented as

$$P_i - \sum_{j=1}^{N} Y_{ij} U_i U_j \cos(\delta_i - \delta_j - \theta_{ij}) = 0, \qquad (2.7)$$

$$Q_i - \sum_{j=1}^{N} Y_{ij} U_i U_j \sin(\delta_i - \delta_j - \theta_{ij}) = 0. \qquad (2.8)$$

Where

P_i is active power at bus i.

Q_i is reactive power at bus i.

Y_{ij} is element of admittance matrix parameter between bus i and j.

θ is angle of Y_{ij}.

Load factor (λ) is used to formulate load flow equations as below:

$$P_{Li} = P_{L0} + \lambda(K_{Li}S_{\Delta base}\cos(\emptyset_i), \tag{2.9}$$

$$Q_{Li} = Q_{L0} + \lambda(K_{Li}S_{\Delta base}\sin(\emptyset_i). \tag{2.10}$$

$$P_{Gi} = P_{Gi}(1 + \lambda K_{Gi}) \tag{2.11}$$

Where

P_{L0}, Q_{L0} is initial active and reactive load demand at bus i.

P_{Li}, Q_{Li} is active and reactive load demand at bus i.

K_{Li} is multiplier to designate the rate of load change at bus i as λ changes.

$S_{\Delta base}$ is given quantity of the apparent power, which is chosen to provide appropriate scaling of λ.

P_{G0} is initial active power generation at bus i.

P_{Gi} is active power generation at bus i.

K_{Gi} is the constant of changing rate in generation.

2.2.3 Optimization method

Optimization method in [2] is used to calculate load margin of the power system by using many optimization techniques, for example, Heuristic searches, Genetic Algorithms, and Tabu search to solve the power flow calculation. Objective function is defined for finding the maximum of the incremental load parameters. This method provides only a boundary point.

$$\text{Minimize} \quad f(x) \tag{2.12}$$

$$\text{Subject to} \quad h(x) = 0, \tag{2.13}$$

$$g(x) \leq 0, \tag{2.14}$$

$$x^{(lb)} \leq x \leq x^{(ub)}. \tag{2.15}$$

Where

$f(x)$ is the objective function of the optimization.

x is variable of the power system which includes bus voltage magnitude, bus voltage angle, power generation and load demand.

$h(x)$ are equality constraints which are power flow equation.

$g(x)$ are inequality constraints which are branch flow limit.

$x^{(lb)}$ are lower limit of the variables.

$x^{(ub)}$ are upper limit of the variables.

2.3 Classification of Security Region

The power flow solution regions in [31] can be classified into 3 regions as shown in Figure 2.3. The unsolvable region is outermost region. This region is the set of points which have no power flow solution because the solution cannot satisfy both power system equality constraints and inequality constraints. Second region is infeasible region. This region is the set of power flow solution points but there is some solution exceed the power system limit constraints and violate to the power system. Lastly, the innermost region is the feasible region. This region is the set of feasible power flow solutions and all solutions must satisfy all power system constraints. In feasible region, the feasible point is used to determined power system operating point and satisfies all power system constraints.

This research considers only the solution from the feasible region which is not violate the power system. The boundary of the feasible region is used to determine maximum load demand. Load points on the boundary are the maximum load demand at that direction.
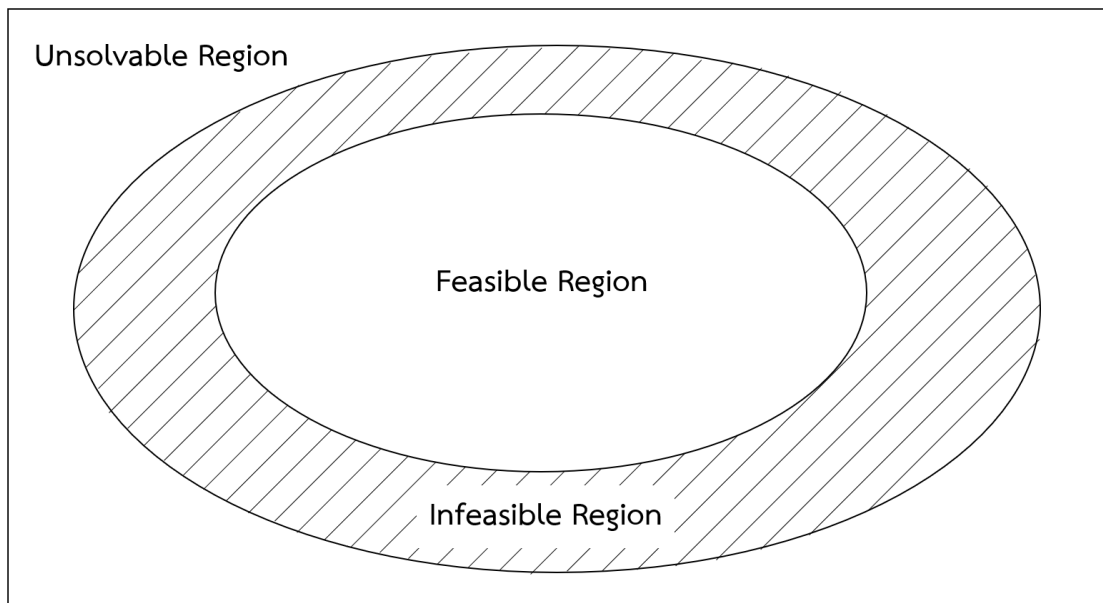
Figure 2.3 Security regions

จุฬาลงกรณ์มหาวิทยาลัย
CHULALONGKORN UNIVERSITY

CHAPTER 3

Load Security Region

Load security region is the power flow solutions set which is on the boundary point and not exceed power system constraints. In addition, the load security region is determined by tracing algorithm in [4]. Tracing algorithm consists of 3 parts. The first part is continuation method. This method is similar to continuous power flow because this method consists of prediction process and correcting process. The second part is optimization-based method which is the correcting process. The last part is initialization process of tracing algorithm. This part is used to calculate initial guess and first prediction point.

3.1 Continuation Method

A set of saddle node bifurcation (SNB) points is contained in the feasible region curve which are the critical points of power flow solutions on the boundary. The SNB points are changed upon the power system parameters and the direction of load expansion which can be obtained by the tracing boundary. Continuation method in [6] includes 2 steps.

3.1.1 Predictor Process

Predictor process is the first step. This process is used to predict the next point (z_p) on the curve to find tangent to the curve at the previous point (z_1) that moves along the vector distance (τ) by the unit vector v. The prediction of the next point on the curve is

$$z_p = z_1 + \tau v. \tag{3.1}$$

3.1.2 Corrector Process

Corrector process is the second step. This process is used to correct a z_p to the next boundary point on curve (z) by,

$$(z - z_p)^t v = 0. \tag{3.2}$$

Equation (3.2) can be reformed as

$$(z - z_1)^t v = \tau. \qquad (3.3)$$

The predictor–corrector process is illustrated in Figure 3.1.
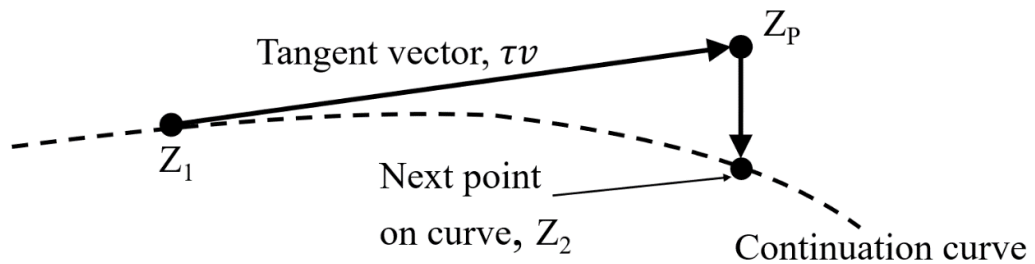
Figure 3.1 Predictor–corrector process

3.1.3 Step size

Predictor process can provide inappropriate prediction point which is inside the feasible region because of inappropriate step size as shown in Figure 3.2. Step size (τ) is defined by tangent vector (τv). Thus, step size is a key factor to determine the load security region. Problem of inappropriate step size has 2 conditions.
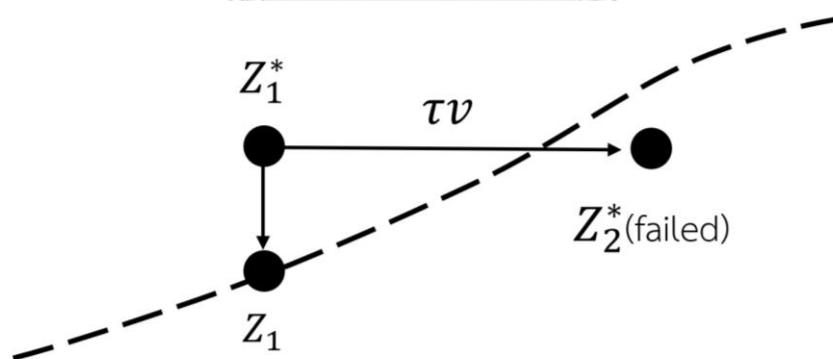
Figure 3.2 Failure prediction point determination

The first problem is too large step size. This problem can break tracing algorithm by providing inappropriate prediction point which is inside the feasible region. Thereby, the inappropriate prediction point must be corrected automatically. Moreover, large step size can reduce the accuracy of the load security region and caused the wide gap as a result of divergent solution. Gap is distance between two

prediction points. The wider gap, the less boundary accuracy. Nonetheless, wide gap can reduce a number of iterations.

The second problem is too small step size. This problem can break tracing algorithm as too large step size. The too small step size is the cause of a lot of iteration. A lot of iteration is the cause of long computation time, especially in the large power system or power system with many variables as a result of not convergence in a specific time. Although, the high boundary accuracy is necessary. The narrower gap, the more computation time. Lastly, the appropriate step size is required.

3.2 Optimization-Based Method

From continuation method, the corrector process is replaced by the optimization-based method in [4]. This process is used to determine the boundary point of the power system solutions. Each boundary point is solved by the conventional power flow equations which are nonlinear equations and nonconvex. Optimization-based method consist of 2 parts. The first part is objective function and the other part is power system constraints.

3.2.1 The Objective Function

The conventional power flow equations consist of equations (2.12-2.15). The objective function in equation (2.12) is written in equation (3.4).

$$\text{Minimize} \quad \frac{1}{2}(S - S^*)^T(S - S^*) \tag{3.4}$$

Where

S^* is the prediction point from the prediction process.

S is the load injection point which is considered.

Let a^T denote the transpose matrix of a.

The feasible region in chapter 2 can be shaped by many power system parameters. The load security region determination is still complicated even a small

power system. This research implements the tests on 2 power transfer aspects. The first aspect considers the power transfer between two buses which are one generator and one load bus. The other power transfer aspect considers between two areas which are a group of generators and a group of load buses whereas one group can be considered from more than one area. Sink is considered load demand which is free variables in the power system. Apart from that, source is considered generation which is free variables in the power system.

Power transfer from source bus to sink bus is the power transfer which is generated from one generation in the source bus then transfer to one load bus in the power system. Other parameters of the power system are fixed. Power flow solutions are active and reactive power demand of the considered load bus. The solutions are visualized on the P-Q plane which x-axis is only active load demand variable and y-axis is only reactive power demand variable.

Power transfer from source area to sink area is similar to power transfer from source bus to sink bus. Source area is the summation of considered generation in the power system. In other words, sink area is the summation of considered load demand. In the power transfer, other generation and load parameters which are not determined are fixed. Power flow solutions of this power transfer is the summation of active load demand and the summation of reactive load demand. Consequently, the solutions are visualized on the P-Q plane as power transfer from source bus to sink bus.

3.2.2 Constraints

The conventional constraints in [29] consist of the equality and inequality constaints which are presented in equation (2.13-2.14) . This equality constraints are used to calculate power flow of the power system. The equation (2.1-2.3) are formulated as below.

$$S_i = (\sum P_{Gi} - \sum P_{Di}) + j(\sum Q_{Gi} - \sum Q_{Di}), \qquad i \in N \qquad (3.5)$$

$$S_i = \sum_{j \sim i} S_{ij}. \qquad\qquad i \in N, i, j \in E \qquad (3.6)$$

Where

S_i is complex power of bus i.

$\sum P_{Gi}$ is the summation of active power generation in bus i.

$\sum P_{Di}$ is the summation of active load demand in bus i.

$\sum Q_{Gi}$ is the summation of reactive power generation in bus i.

$\sum Q_{Di}$ is the summation of reactive load demand in bus i.

S_{ij} is complex branch flow from bus i to bus j.

i is from bus.

j is to bus and not equal to from bus.

N is total bus in the power system.

E is total branch in the power system.

The complex branch power (S_{ij}) is expressed as

$$S_{ij} = U_i I_{ij}^H \qquad\qquad i,j \in E \qquad (3.7)$$

$$I_{ij} = (U_i - U_j)Y_{ij} + j\frac{B_c}{2}U_i \qquad\qquad i,j \in E \qquad (3.8)$$

$$S_{ij} = Y_{ij}^H U_i U_i^H - Y_{ij}^H U_i U_j^H - j\frac{B_c}{2}U_i U_i^H \qquad\qquad i,j \in E \qquad (3.9)$$

$$S_{ji} = Y_{ij}^H U_j U_j^H - Y_{ij}^H U_j U_i^H - j\frac{B_c}{2}U_j U_j^H \qquad\qquad i,j \in E \qquad (3.10)$$

$$S_{ij} = P_{ij} + jQ_{ij} \qquad\qquad i \in N \qquad (3.11)$$

$$P_{ij} = G_{ij}U_i{}^2 - G_{ij}U_i U_j \cos(\delta_{ij}) + B_{ij}U_i U_j \sin(\delta_{ij}) \quad i \in N, i,j \in E \qquad (3.12)$$

$$Q_{ij} = B_{ij}U_i{}^2 - B_{ij}U_i U_j \cos(\delta_{ij}) - G_{ij}U_i U_j \sin(\delta_{ij}) - \frac{B_c}{2}U_i{}^2 \quad i \in N, i,j \in E \quad (3.13)$$

Where

B_c is shunt susceptance.

I_{ij} is the current flow from bus i to bus j.

P_{ij} is the active branch flow from bus i to bus j.

Q_{ij} is the reactive branch flow from bus i to bus j.

G_{ij} is the real parts of the admittance matrix element Y_{ij}.

B_{ij} is the imaginary parts of the admittance matrix element Y_{ij}.

B_c is shunt susceptance

The power system element is represented by a line model as shown in Figure 3.3.

Figure 3.3 Line model
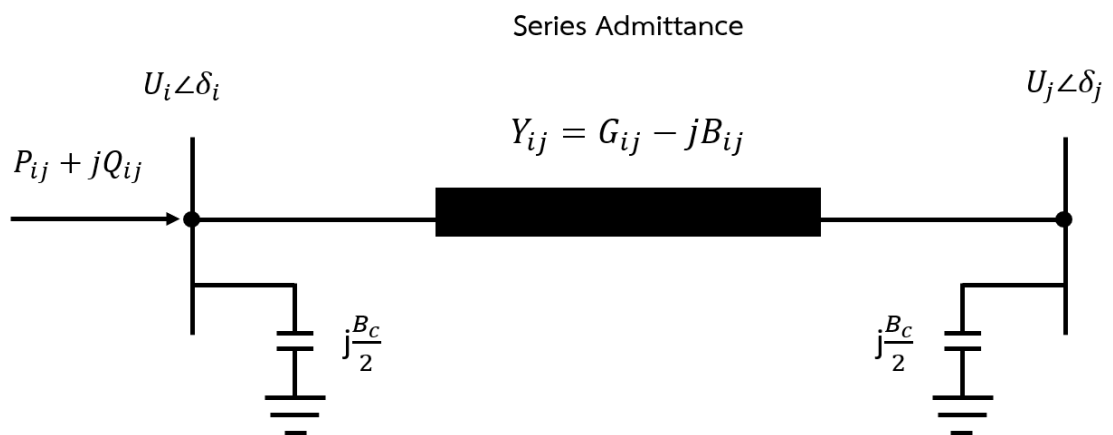
The inequality constraints are used to set the branch flow limit. The equation (2.14) is express as below.

$$|S_{ij}| \leq S_{ij}^{max} \quad i,j \in E \tag{3.14}$$

$$|S_{ji}| \leq S_{ij}^{max} \quad i,j \in E \tag{3.15}$$

Where S_{ij}^{max} is the rated branch flow for branch ij.

From the corrector process in section 3.1, the optimization-based method is used to solve the optimization problem and obtain the boundary point. The objective function value is represented as the shortest distance from the prediction point (S^*) to the boundary point (S) which is power flow solutions on the feasible region. The next prediction point is calculated by using the perpendicular vector v from Figure 3.4. This vector is perpendicular to the vector $S - S^*$. From vector operation of perpendicular vector, vector v is defined as follow.

$$(S_n - S_n^*)^T v_n = 0 \tag{3.16}$$

Where n is iteration round.
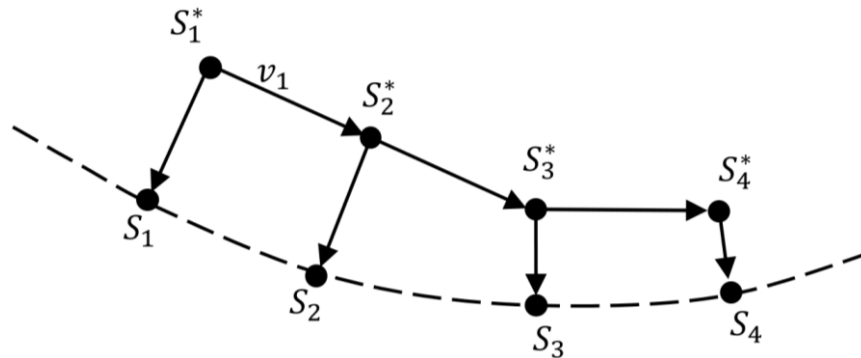
Figure 3.4 Load security region by tracing algorithm

3.2.3 The Prediction Point inside the Region

From Figure 3.4, predictor process from section 3.1.1 must determine the next prediction point S_{n+1}^* from the previous point S_n^*. However, predictor process can provide an inappropriate prediction point which is inside the feasible region as describe in section 3.1.3. This section explains the important of prediction point location.

The prediction point location must be outside of the feasible region. When the prediction point is inside the feasible region, the corrector process cannot operate forasmuch as the objective function value is the shortest distance from outside of the feasible region to boundary of the feasible region. The objective function value is always equal to zero as a result the solution from power system is always optimized but the solution is not the boundary of the feasible region. Consequently, the incorrect solutions are still provided in the next iteration of tracing algorithm.

3.3 Initial Guess and First Prediction Point

Initial guess and prediction point are the first step of tracing algorithm. The initial guess is power flow solutions set on the boundary. The first prediction point is used in first iteration of the algorithm. The initial guess and first prediction point can be determined by several methods. Load margin determination from chapter 2 is used to obtain the maximum load point of the power system. This research applies repeated power flow with bisection method for providing initial guess and first prediction point.

Repeated power flow with bisection method is used to obtain initial guess and first prediction point by increasing load demand until power system parameter reach the constraint. The initial guess is the set of power flow solution at the limit point of the power system constraint. Then, first prediction point is defined from the maximum load point by expanding load margin with appropriated size of load demand.

Initial guess is the first power flow solution set on the boundary. The first prediction point is the point which is outside the feasible region. The corrector process uses prediction points to obtain the shortest distance between prediction points on the boundary point of the feasible region. Furthermore, prediction point must not too far from the load security region.

3.4 Boundary Tracing Method

3.4.1 Repeated Power Flow with Bisection Method

Tracing algorithm uses continuation method to visualize the load security region. Continuation method consists of predictor process and corrector process. Thereby, tracing algorithm must initialize with the first prediction point (S_1^*) and initial guess (X^0). The first prediction point is the first point which is outside the load security region. Initial guess is the set of power flow solution within power system constraints and near the boundary. Repeated power flow with bisection method is used to obtain the first prediction point and initial guess. This method is used to increase load demand from load demand of the base case (S^0) as long as power system parameters reach the power system limit and violation occurs. The load demand is increased by step size σ MVA in direction angle (θ). As a result, the first prediction point which is infeasible point is obtained and initial guess which consists of power flow solutions at the boundary point (S^b) is obtained. Repeated power flow method is presented in Figure 3.5.
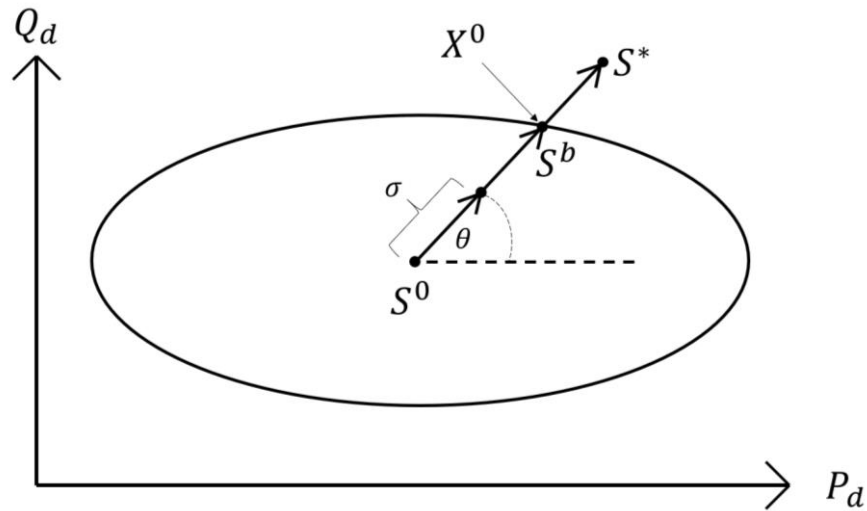
Figure 3.5 Process to determine first infeasible point

The first infeasible point and solutions on the boundary point are determined by using the repeated power flow method as following steps.

1. k is defined as step iteration number and k is set to 1 for the first step.

2. σ is defined as step size of the load increment.

3. The load demand of the base case is defined as S^0 and the direction angle is defined as θ.

$$S^0 = P_d^0 + jQ_d^0 = \sum_{i=1}^{n} P_{di}^0 + j\sum_{i=1}^{n} Q_{di}^0 \tag{3.17}$$

$$P_d^k = P_d^0 + (k\sigma\cos\theta) \tag{3.18}$$

$$Q_d^k = Q_d^0 + (k\sigma\sin\theta) \tag{3.19}$$

4. Solve the power flow equation with load incremental from step 3.

5. Examine the power flow solutions. If the solutions do not exceed the power system constraints, then return to step 3 and add k by 1. If solutions exceed the power system constraint, then move to the next step.

6. Case A is the case which is not violate the power system constraints and case B is the case which violates the power system constraints. The load demand of case A and B is defined as follow.

Case A: $P_d^A = P_d^{k-1}, Q_d^A = Q_d^{k-1}$,and $S_d^A = P_d^A + jQ_d^A$

Case B: $P_d^B = P_d^{k-1}, Q_d^B = Q_d^{k-1}$,and $S_d^B = P_d^B + jQ_d^B$

7. The difference between S^A and S^B is defined as $\left| S^A - S^B \right|$ and the threshold is ε. If $\left| S^A - S^B \right|$ is less than ε, then move to next step. If $\left| S^A - S^B \right|$ is greater than ε, then move to step 10.

8. Case C is defined as follow.

$$P_d^C = \frac{1}{2}\left(P_d^B - P_d^A\right). \tag{3.20}$$

$$Q_d^C = \frac{1}{2}\left(Q_d^B - Q_d^A\right). \tag{3.21}$$

9. Determine the power flow solutions of the case C. If the solutions of case C are satisfying all power system constraints, Let $P_d^A = P_d^C$ and $Q_d^A = Q_d^C$. If the solutions of case C violate the power system constraint, Let $P_d^B = P_d^C$ and $Q_d^B = Q_d^C$. After that return to step 7.

10. S^A is set to the boundary point S^b and the power flow solutions set is set to the initial guess X^0.

11. The prediction point is defined as below.

$$S^* = S^b + \mu \frac{(S^b - S^0)}{|S^b - S^0|} \tag{3.22}$$

Where is μ the step size.

The repeated power flow with bisection method is summarized as the flowchart below.
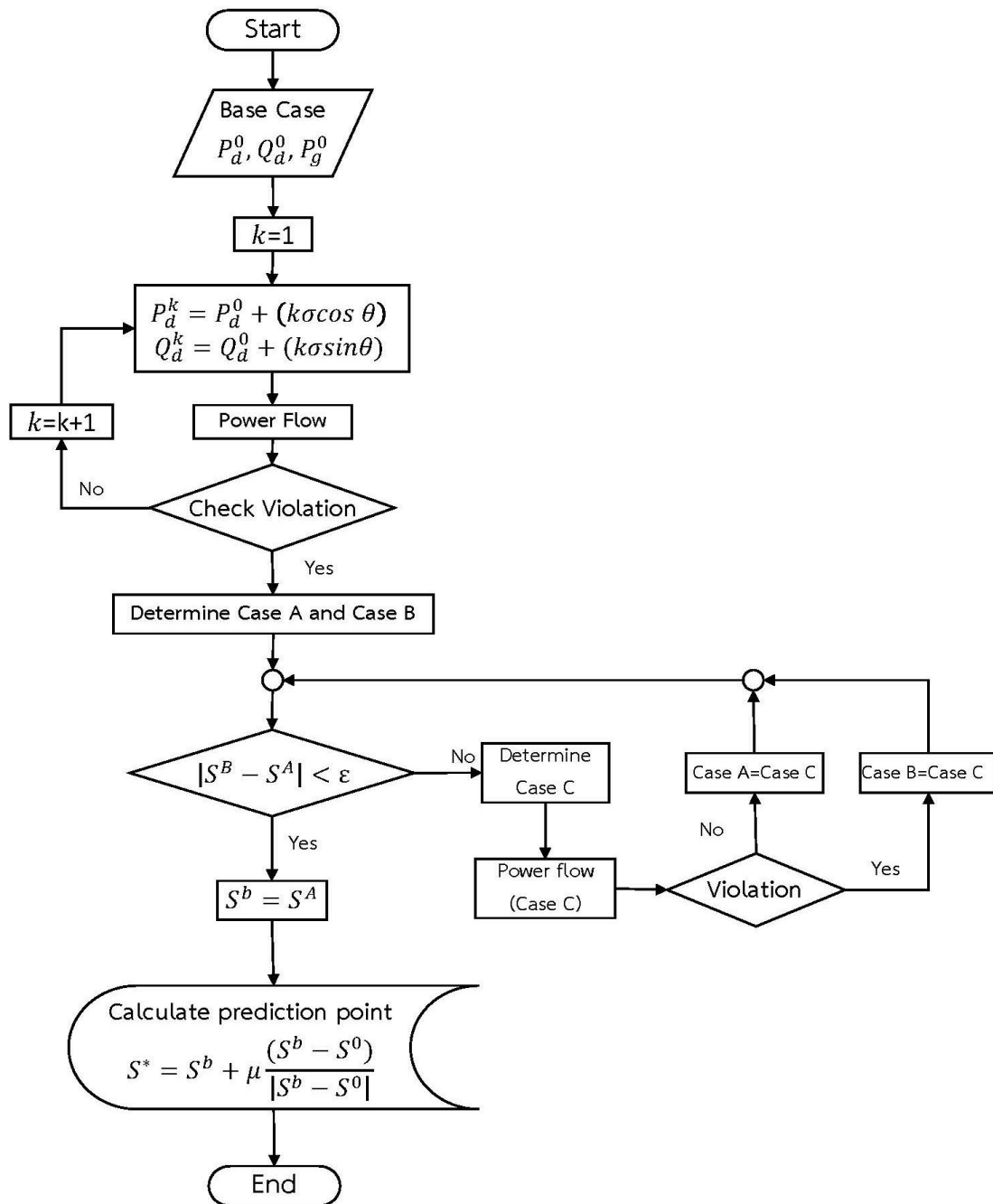
Figure 3.6 Flowchart of repeated power flow with bisection method

3.4.2 Corrector Process

The corrector process is used in the optimization problem as explain in the tracing algorithm in the section of optimization-based method. From the previous section, the corrector process uses prediction point from predictor process to find the power flow solutions point on the boundary. The prediction points are separated into 2 cases.

The first case of the prediction point is appropriate prediction point. Corrector process can use the prediction point of the first case. The objective function value is greater than 0 in this case. The other case of the prediction point is inappropriate prediction point. Corrector process cannot use the prediction point of the case because this prediction point is inside the feasible region. For this reason, the objective function value always equal to 0 that mean the correction point is the same point of the prediction point. Therefore, corrector process can obtain the power flow solutions, but this method fails to obtain the solution on the boundary point.

This section is proposed to modify the inappropriate prediction point which is inside the feasible region to the appropriate point which is outside the feasible region. A new prediction point is represented by following equation.

$$S_k^{*(new)} = S_k^* + \left[\frac{S_{k-1}^* - S_{k-1}^b}{|S_{k-1}^* - S_{k-1}^b|} \times \rho \right] \tag{3.23}$$

Where

$S_k^{*(new)}$ is modified prediction point of the iteration k.

S_k^* is inappropriate prediction point of the iteration k.

S_{k-1}^* is the prediction point of the iteration k-1 or the previous prediction point.

S_{k-1}^b is the power flow solution on the boundary point.

ρ is an adjusted size.

This process is repeated whenever $S_k^{*(new)}$ is the appropriate point which is not inside the feasible region as shown in figure below.
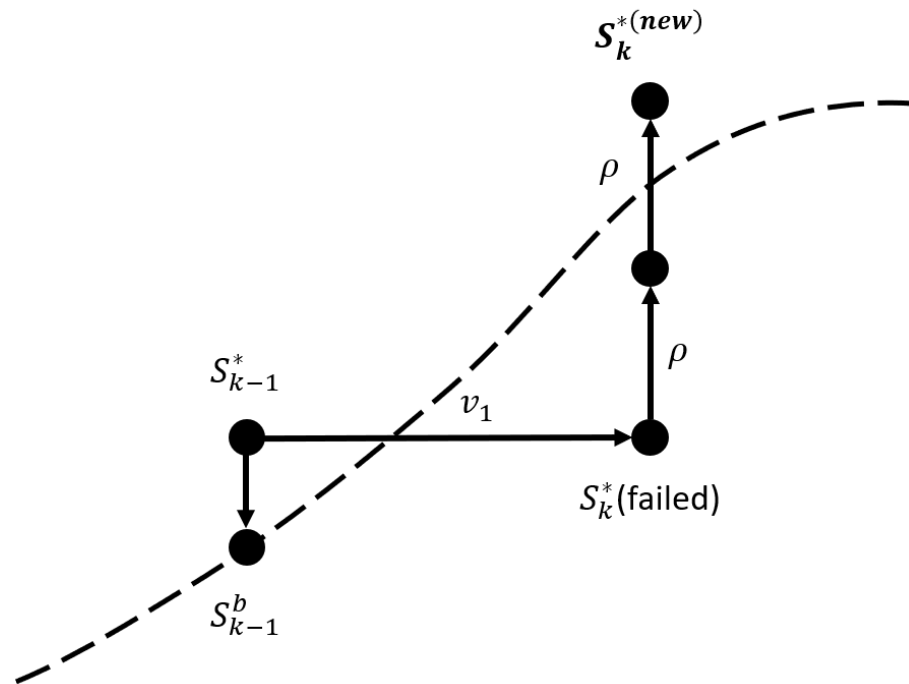
Figure 3.7 The process to modify the inappropriate prediction point

3.4.3 Predictor Process

The predictor process is used to predict the next prediction point to be used in the corrector process. The next prediction points are determined by continuation method. This process must be adjusted the distance gap between the prediction point to the boundary point. The research proposes method to adjust a gap as below.

$$S_k^{*\prime} = S_k^b + \left[\frac{S_k^b - S_k^*}{|S_k^b - S_k^*|} \times d \right]$$ (3.24)

Where

$S_k^{*\prime}$ is previous prediction point at iteration k which distance gap between prediction point and the boundary point is d.

d is the adjusted distance gap.

Then, the next prediction point is calculated by equation (3.25-3.26).

$$S^*_{k+1} = S^{*\prime}_k + l \cdot \Delta S^*_k \qquad (3.25)$$

$$\Delta S^*_k = j \times \frac{S^b_k - S^*_k}{|S^b_k - S^*_k|} \qquad (3.26)$$

Where

S^*_{k+1} is next prediction point.

l is a scalar step size parameter.

ΔS^*_k is the perpendicular vector.

The adjusted predictor process is presented as Figure 3.8.
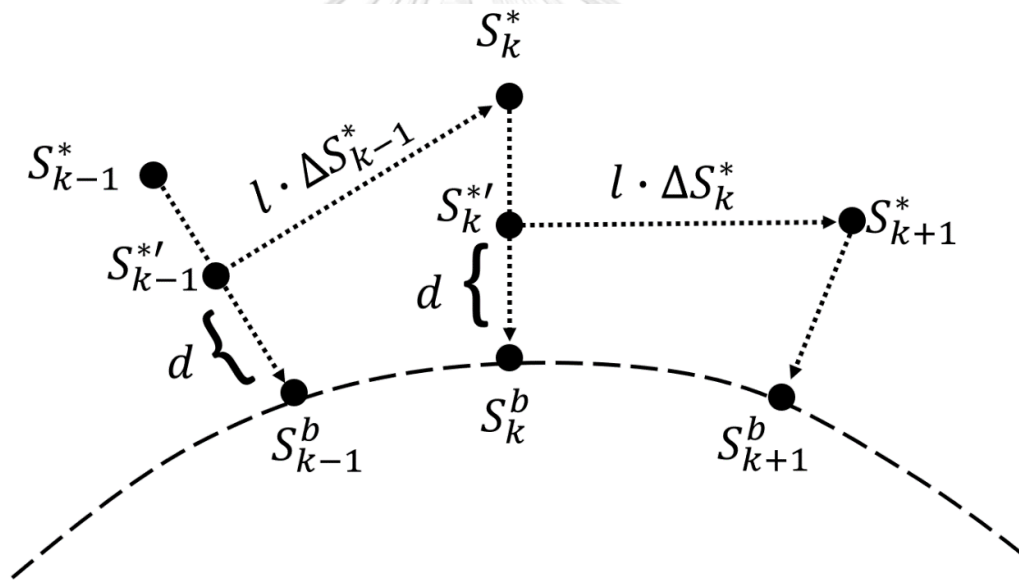
Figure 3.8 The adjusted predictor process

3.4.4 Tracing Algorithm

This section summarizes all tracing algorithm as the following step.

1. Determine the first prediction point and the initial guess by repeated power flow with bisection method.
2. Set $k = 1$ for the first iteration.
3. Using optimization-based method to obtain the power flow solution point S_k^b on the boundary and others parameter X_k.
4. Test the prediction point S_k^* by optimization. If S_k^* is inside the feasible region by $S_k^* = S_k^b$, then modify the prediction point in step 5. If $S_k^* \neq S_k^b$, then move to step 6.
5. Calculate new prediction point by the process in section 3.4.2 and repeated step 3.
6. The load security region examining is closed region or not. If the region is not closed, then repeat tracing algorithm in step 7. If the region is completely closed, then stop tracing algorithm.
7. Record the power flow solution of the boundary point X_k. Then, X_k is used to set as initial guess X_{k+1}^0 to determine in the next iteration.
8. Calculate the next prediction point by the method in section 3.4.3.
9. Start the next iteration. Return to step 3 and adding k by 1.

The tracing algorithm is summarized in the flowchart as Figure 3.9. Load security region is visualized as shown in the Figure 3.10.
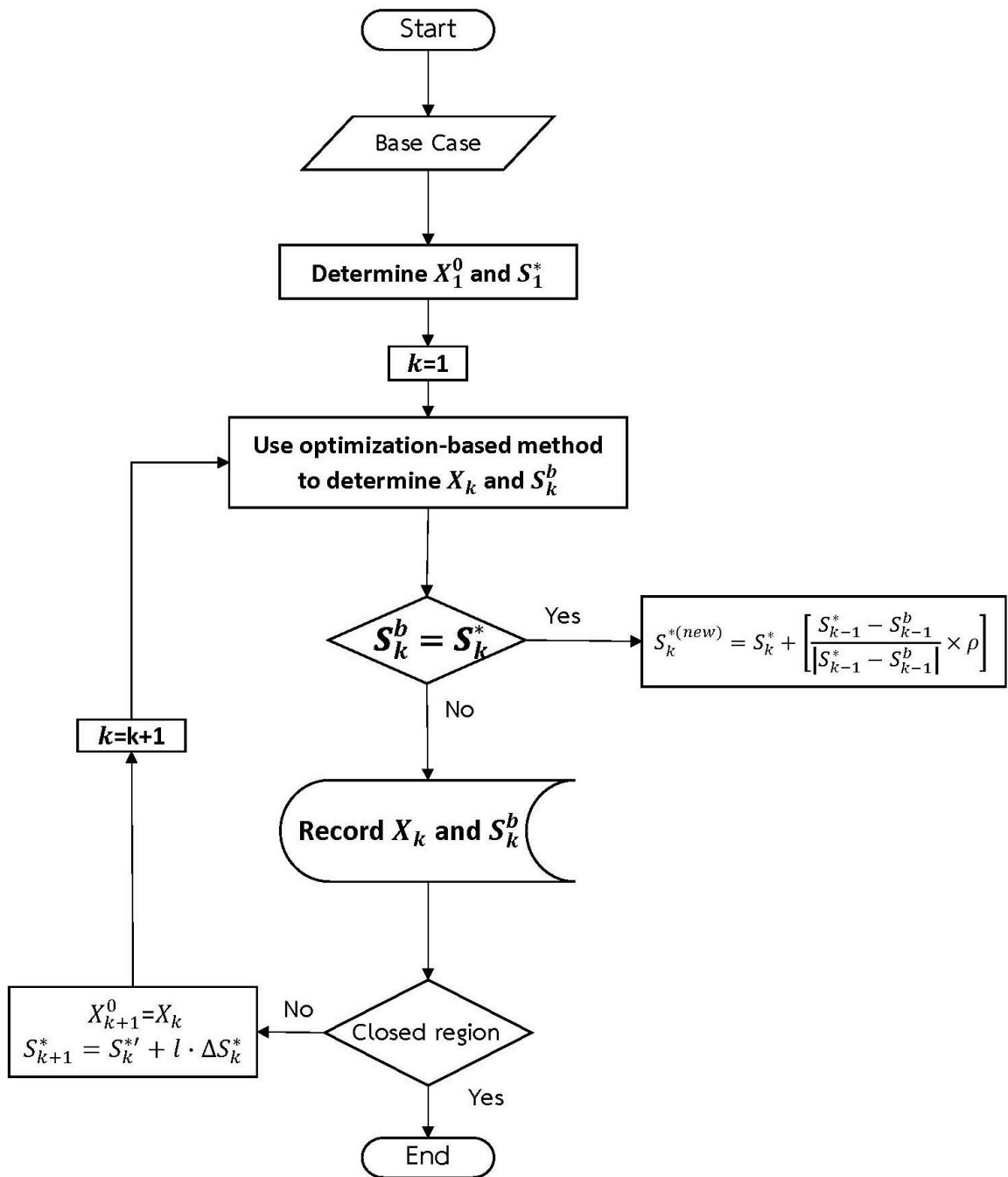
Figure 3.9 Flow chart of tracing algorithm
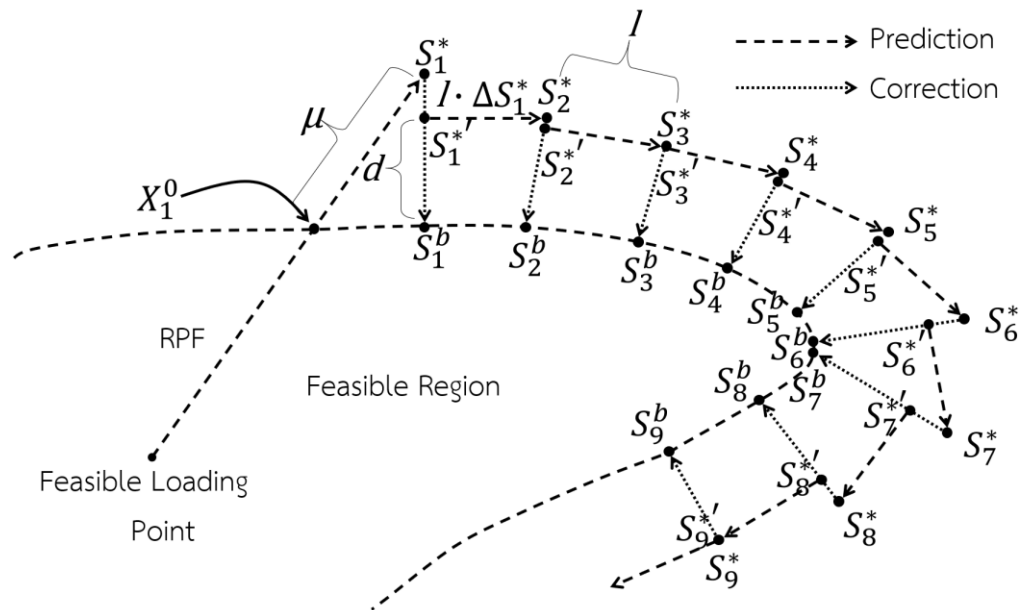
Figure 3.10 Visualized load security region

CHAPTER 4

Tracing Algorithm with SOCP Relaxation

Optimization-based method from tracing algorithm is based on the alternating current optimal power flow (ACOPF). The ACOPF is the foundation of the power system analysis. The ACOPF is used to find the optimal solution from the objective function, such as grid planning, loss minimization, and load margin. The ACOPF is a nonconvex optimization problem and NP-hard in [9] so a feasible solution is challenging problem. The challenges of solving ACOPF problem are 2 aspects. The first aspect is the computation time and the other is nonconvex optimization problem on a large-scale power system.

Several methods are proposed to solve the ACOPF problem. These methods are classified into several categories, such as,

1. Approximated methods in [10]-[12]
2. Non-linear optimization methods in [13]-[15]
3. Heuristic methods in [16]-[17]
4. Convexification approaches in [5].

This work proposes relaxation from convexification approach. Second-order cone program (SOCP) relaxation is applied to solve the ACOPF problem. This chapter describes basic SOCP, SOCP relaxation, and exactness of SOCP.

4.1 Basic SOCP

Convex conic programs in [32] are polynomial solvable. To convexify, semidefinite program (SDP) relaxation is applied to find the global optimal solution of the ACOPF problem. SDP consists of linear matrix inequalities. However, the SDP relaxations can determine only for some assumptions, but this relaxation is not effective in the large-scale power system. Therefore, SOCP relaxation is used to reduce computation time instead of SDP in the large-scale power system because SOCP can

be solved by interior point method which is more efficiently than SDP problem. This section explains the key factor of the SOCP relaxation.

SOCP is a linear function which the objective function is minimized though the intersection of the product of second-order cones and affine set. Additionally, SOCP can be reduced to several convex optimization problems classes, such as linear programing (LP), quadratic program (QP), and quadratically constrained quadratic program (QCQP). Nevertheless, SOCP is less general than SDP. Classic second-order cone program is a convex optimization problem which is expressed as the form below.

Minimize $\quad f^T x$

Subject to $\quad \|A_i x + b_i\|_2 \le c_i^T x + d_i \qquad\qquad i \,\epsilon\, 1, \dots, N$ $\qquad\qquad$ (4.1)

$\qquad\qquad\quad F x = g$

Where $x \in R^n$ is defined as the optimization variable, the optimization problem parameters are $f \in R^n$, $A_i \in R^{(n_i-1) \times n}$, $b_i \in R^{n_i}$, $c_i \in R^n$, $d_i \in R$, and $F \in R^{p \times n}$. The norm $\|x\|_2$ is the standard Euclidean norm and a^T indicates transpose.

SOCP constraint is equivalent to a linear matrix inequality from SDP. For this reason, SOCP can be formulated as SDP.

Minimize $\quad f^T x$

Subject to $\quad \begin{bmatrix} (c_i^T x + d_i)I & A_i x + b_i \\ (A_i x + b_i)^T & c_i^T + d_i \end{bmatrix} \succeq 0 \qquad\qquad i \,\epsilon\, 1, \dots, N$ $\qquad\qquad$ (4.2)

Although, SOCP can formulate as SDP but solving SOCP though SDP is not suitable. SOCP can be solved by Interior point methods which are many solvers, such as fmincon and CVX. These solvers can solve the optimization problem directly to the SOCP problem class not to general class like SDP. As a result, the number of iterations is reduced. A constant fraction in [33] is bounded by $O(\sqrt{\sum_i n_i})$ for SDP and $O(\sqrt{N})$ for SOCP. Furthermore, each SOCP iteration is faster than SDP because SOCP work per iteration is $O(n^2 \sum_i n_i)$ and SDP is $O(n^2 \sum_i n_i^2)$.

SOCP can be solved very efficiently by primal-dual interior-point in [33]. This method is more efficient than casting the SOCP to SDP problem. From equation (4.1), SOCP is simplified by notation as follow.

$$u_i = A_i x + b_i \qquad i = 1, \ldots, N \qquad (4.3)$$

$$t_i = c_i^T x + d_i \qquad i = 1, \ldots, N \qquad (4.4)$$

SOCP problem is rewritten as below.

Minimize $\quad f^T x$

Subject to $\quad \|u_i\| \le t_i \qquad\qquad i = 1, \ldots, N \qquad (4.5)$

$\qquad\qquad u_i = A_i x + b_i \qquad i = 1, \ldots, N$

$\qquad\qquad t_i = c_i^T x + d_i \qquad i = 1, \ldots, N$

Additionally, the dual of the SOCP is presented as follow.

Minimize $\quad -\sum_{i=1}^{N}(b_i^T z_i + d_i w_i)$

Subject to $\quad \sum_{i=1}^{N}(A_i^T z_i + c_i w_i) = f \qquad i = 1, \ldots, N \qquad (4.6)$

$\qquad\qquad \|z_i\| \le w_i \qquad\qquad\qquad i = 1, \ldots, N$

Where $z_i \in R^{n_i-1}$ is the dual optimization variables, $w \in R^N$ by $i = 1, \ldots, N$

The dual SOCP is a complex problem where the objective function is concave, and constraints are convex. The equation (4.6) is the same format as the equation (4.5). To eliminate the equality constraints, this work recasts the dual SOCP in the same format as the classic SOCP from equation (4.1).

The classic SOCP is treated as the primal SOCP from equation (4.1). The primal SOCP is divided into 2 aspects. The first is feasible and the other is strictly. The primal SOCP is feasible when the exists primal feasible x satisfies all power system constraint, otherwise the primal SOCP is strictly feasible when the exists strictly primal feasible x satisfies the constraints with strict inequality. p^* is defined as the optimal value of the primal SOCP. This problem is infeasible when $p^* = +\infty$. In addition, the vectors z and

w from the dual SOCP is divided into 2 aspects. The first is dual feasible and the other is strictly dual feasible. The vectors z and w are dual feasible when these satisfy all power system constraints. On the other hand, the vectors z and w are strictly dual feasible when these satisfy $\|z_i\| < w_i, i = 1, ..., N$. d^* is defined as the optimal value of the dual SOCP. This problem is infeasible when $d^* = +\infty$.

The dual problem is separated as following conditions,

1. Weak duality where $p^* \geq d^*$,
2. Strong duality when the primal or dual problem is strictly feasible where $p^* = d^*$,
3. The optimal value is obtained when the primal and dual problems are strictly feasible which exist primal and dual feasible point.

4.2 Optimization-based Method with SOCP Relaxation

From Optimization-Based Method section in chapter 3, this optimization problem are nonlinear equation and nonconvex problems which is hard problem and hard to obtain global optimal solution. For this reason, this method is computationally expensive and intractable. This work proposes second order cone program (SOCP) relaxation in [5] to solve optimization problem within polynomial time. SOCP relaxation is to formulate the optimization problem as convex optimization which is cone format. This method consists of 2 steps as shown in Figure 4.1.

Optimal Power Flow Problem

First Step

Power flow equations without current variables

Second Step

Nonconvex equations changed into convex inequations
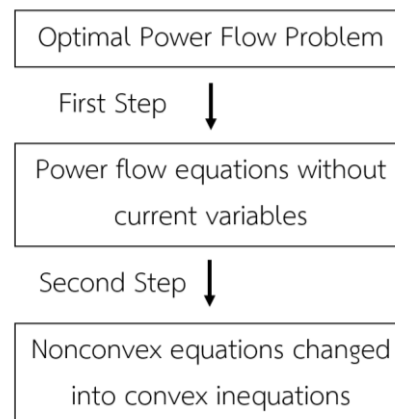
Figure 4.1 SOCP relaxation process

4.2.1 First Step of Optimization-Based Method with SOCP Relaxation

The first step of relaxation is used to eliminate the nonconvex term in equation (3.9-3.10). This method defined new variables of the bus voltage production terms which is the same bus term as follow.

$$V_i = U_i U_i^H \qquad\qquad i \in N \qquad (4.7)$$

This works defines new variables for the different bus voltage production terms as below.

$$V_{ij} = U_i U_j^H \qquad\qquad i, j \in E \qquad (4.8)$$

The proposed optimization constraints are formulated as follow.

$$S_{ij} = Y_{ij}^H V_i - Y_{ij}^H V_{ij} - j\frac{B_c}{2} V_i \qquad (4.9)$$

$$S_{ji} = Y_{ij}^H V_j - Y_{ij}^H V_{ij}^H - j\frac{B_c}{2} V_j \qquad (4.10)$$

The equality constraints in convex optimization problem must be affine but V_{ij} from equation (4.9)–(4.10) is not affine. For this reason, V_{ij} is defined with new complex term as below.

$$\left|V_{ij}\right|^2 = V_i V_j \qquad (4.11)$$

$$V_{ij} = a_{ij} + jb_{ij} \qquad (4.12)$$

$$a_{ij} = U_i U_j \cos(\delta_{ij}) \qquad (4.13)$$

$$b_{ij} = U_i U_j \sin(\delta_{ij}) \qquad (4.14)$$

Where

a_{ij} is real part of V_{ij}.

b_{ij} is imaginary part of V_{ij}.

Equation (3.12)–(3.13) from chapter 3 is formulated by using a_{ij} and b_{ij} from equation (4.13)–(4.14). Hence, the branch flow is represented in equation (4.15-4.18).

$$P_{ij} = G_{ij}(V_i - a_{ij}) + B_{ij}b_{ij} \tag{4.15}$$

$$P_{ji} = G_{ij}(V_j - a_{ij}) - B_{ij}b_{ij} \tag{4.16}$$

$$Q_{ij} = -G_{ij}b_{ij} + B_{ij}(V_i - a_{ij}) - \frac{B_c}{2}V_i \tag{4.17}$$

$$Q_{ji} = G_{ij}b_{ij} + B_{ij}(V_j - a_{ij}) - \frac{B_c}{2}V_j \tag{4.18}$$

The equation (4.11) is expressed by using a_{ij} and b_{ij} as

$$a_{ij}^2 + b_{ij}^2 = V_iV_j \tag{4.19}$$

In additionally, V_i are set the upper and lower bound to obtain equivalent as the conventional optimization problem as follow.

$$U_{min}^2 \leq V_i \leq U_{max}^2 \qquad i \in N \tag{4.20}$$

$$V_i = U_{ref}^2 \qquad i \in N \tag{4.21}$$

Where U_{ref} is defined as the slack bus voltage.

4.2.2 Second Step of Optimization-Based Method with SOCP Relaxation

The second step of relaxation is used to apply to quadratic equation and formulate the problems as convex problem. Equation (4.19) is quadric equation. This step is used to reform that equation into rotating cone by relaxation. The relaxation is the method to relax equality sign to inequality sign as below.

$$a_{ij}^2 + a_{ij}^2 \leq V_iV_j \tag{4.22}$$

Equation (4.22) can be shown as a cone in a 2-norm form.

$$\left\| \begin{matrix} 2a_{ij} \\ 2b_{ij} \\ V_i - V_j \end{matrix} \right\|_2 \leq V_i + V_j \tag{4.23}$$

The equation (4.23) is inequality constraint which is formulated as conic format.

The classic optimization problems are transformed from nonlinear and nonconvex problem to convex problem. The proposed optimization formulation with SOCP relaxation can be summarized as follow.

Minimize $\qquad \frac{1}{2}\{(\sum_{i=1}^{n} P_{di} - P_{di}^*)^2 + (\sum_{i=1}^{n} Q_{di} - Q_{di}^*)^2\}$

Subject to $\qquad P_{gi} + P_{di} = \sum_{j \sim i} P_{ij}$

$$Q_{gi} + Q_{di} = \sum_{j \sim i} Q_{ij}$$

$$P_{ij} = G_{ij}(V_i - a_{ij}) + B_{ij}b_{ij}$$

$$P_{ji} = G_{ij}(V_j - a_{ij}) - B_{ij}b_{ij}$$

$$Q_{ij} = -G_{ij}b_{ij} + B_{ij}(V_i - a_{ij})$$

$$Q_{ij} = G_{ij}b_{ij} + B_{ij}(V_i - a_{ij}) \qquad (4.24)$$

$$\left\| \begin{matrix} 2a_{ij} \\ 2b_{ij} \\ V_i - V_j \end{matrix} \right\|_2 \le V_i + V_j$$

$$P_{ij}^2 + Q_{ij}^2 \le (S_{ij}^{max})^2$$

$$P_{ji}^2 + Q_{ji}^2 \le (S_{ij}^{max})^2$$

$$U_{i,min}U_{j,min} \le a_{ij} \le U_{i,max}U_{j,max}$$

$$U_{min}^2 \le V_i \le U_{max}^2$$

$$P_{min} \le P_{gi} \le P_{max}$$

$$Q_{min} \le Qg_i \le Q_{max}$$

$$P_{di} \le 0$$

4.3 SOCP Relaxation Exactness

From the second step of optimization-based method with SOCP relaxation, relaxation method is used in equation 4.22. This method transforms the equality constraints to inequality constraints by relax the sign. Equality constraints are more complicated to solve than inequality constraints. Therefore, this section proves the exactness of SOCP relaxation in [30]. Firstly, this works defined a set of optimal solution, a_{ij}, b_{ij}, V_i, and V_j on the branch $i \sim j$ where $i, j \ne 0$ but exclude the distinct line $k \sim l$. That means $\{i, j\} \cap \{k, l\} \ne \emptyset$. So, this relation can be derived as

$$a_{ij}^2 + b_{ij}^2 = V_iV_j \qquad \text{where} \quad \{i, j\} \ne \{k, l\} \qquad (4.25)$$

$$a_{ij}^2 + b_{ij}^2 < V_iV_j \qquad \text{where} \quad \{i, j\} = \{k, l\} \qquad (4.26)$$

Variables on the branch $k \sim l$ is defined as

$$a_{kl}^* = \sqrt{V_k V_l - b_{kl}} \tag{4.27}$$

$$b_{kl}^* = b_{kl} \tag{4.28}$$

$$V_k^* = V_k \tag{4.29}$$

$$V_l^* = V_l \tag{4.30}$$

The related variables are defined with a_{kl}^*, b_{kl}^*, V_k^*, and V_l^* as follow.

$$P_{kl}^* = G_{kl}(V_k^* - a_{kl}^*) + B_{kl} b_{kl}^* \tag{4.31}$$

$$P_{lk}^* = G_{kl}(V_l^* - a_{kl}^*) + B_{kl} b_{kl}^* \tag{4.32}$$

$$Q_{kl}^* = -G_{kl}\, b_{kl}^* + B_{kl}(V_k^* - a_{kl}^*) - \frac{B_c}{2} V_k^* \tag{4.33}$$

$$Q_{lk}^* = G_{kl}\, b_{kl}^* + B_{kl}(V_l^* - a_{kl}^*) - \frac{B_c}{2} V_l^* \tag{4.34}$$

Since $a_{ij}^2 + b_{ij}^2 < V_k V_l$, a_{kl}^* is larger than a_{kl}. Then

$$P_{kl}^* - P_{kl} = G_{kl}(V_k^* - a_{kl}^*) + B_{kl} b_{kl}^* - G_{kl}(V_k - a_{kl}) - B_{kl} b_{kl}$$

$$= G_{kl}(a_{kl}^* - a_{kl}) < 0 \tag{4.35}$$

$$Q_{kl}^* - Q_{kl} = -G_{kl} b_{kl}^* + B_{kl}(V_k^* - a_{kl}^*) + G_{kl} b_{kl} - B_{kl}(V_k - a_{kl})$$

$$= B_{kl}(a_{kl}^* - a_{kl}) < 0 \tag{4.36}$$

From the previous equation (4.35-4.36), the power transfer on branch is represented by the term of power injection as below.

$$P_{Gk}^* - P_{Dk}^* = P_{kl}^* + \sum_{k* \sim i} P_{ki}^*$$

$$= P_{kl}^* + \sum_{k* \sim i} P_{ki} \tag{4.37}$$

$$< P_{Gk} - P_{Dk}$$

$$P_{Gl}^* - P_{Dl}^* = P_{lk}^* + \sum_{l* \sim i} P_{li}^*$$

$$= P_{lk}^* + \sum_{l* \sim i} P_{ki} \tag{4.38}$$

$$< P_{Gl} - P_{Dl}$$

$$Q^*_{Gk} - Q^*_{Dk} = Q^*_{kl} + \sum_{k*\sim i} Q^*_{ki}$$

$$= P^*_{kl} + \sum_{k*\sim i} P_{ki} \qquad (4.39)$$

$$< P_{Gk} - P_{Dk}$$

$$Q^*_{Gl} - Q^*_{Dl} = Q^*_{lk} + \sum_{l*\sim i} Q^*_{li}$$

$$= Q^*_{lk} + \sum_{l*\sim i} Q_{ki} \qquad (4.40)$$

$$< Q_{Gl} - Q_{Dl}$$

When active and reactive load demand still be certain at bus k and l, so $P^*_{Gk} < P_{Dk}$, $P^*_{Gl} < P_{Dl}$, $Q^*_{Gk} < Q_{Dk}$,and $Q^*_{Gl} < Q_{Dl}$,respectively. When P_G and Q_G reached the minimum limit, which is P_{Gmin} and Q_{Gmin}, this method changes the value of P_{Di} and Q_{Di} owing to no maximum limit which is P_{Dmax} and Q_{Dmax}. The values of P_{Gi} and Q_{Gi} still be certain then they will satisfy the power system constraints. This concludes the proof.

CHAPTER 5

Effect of system parameters

From the base case, the load security region is determined by using the tracing algorithm with second order cone programing (SOCP) relaxation. The source area is set from all generation and the sink area is set from considered buses. This chapter describes the load security region variation. The load security region can be varied upon several factor, such as, generation interruption, load shedding, distributed generation (DG) installation in [36] and other device installation. This variation can expand or shrink load security region. This work focuses only the effect of load shedding and photovoltaic (PV) installation.

5.1 Load security region variation

The load security region on the P-Q plane is a set of feasible power flow solution of the sink area. While this work determines the load security region from source area to sink bus, load demand of another load bus can be varied due to load demand variation. Thus, power system operating point will move because of load demand variation and var compensation. This load change does not affect to load security region shape.

The load security region shape can be expanded and shrink by effect of system parameters. System parameters in this chapter includes all power system variables and additional devices. Additionally, the load security region from source area to sink area can be varied from electrical device installation, such as, PV installation and another undesirable situation. However, the loading point is possibly out of the feasible region. The power system operation must bring the power system back by using control action. Control load is method which responses the effect of system parameter, such as, shedding in sink area and generating power from PV generation in source area. The control action is shown in Figure 5.1.
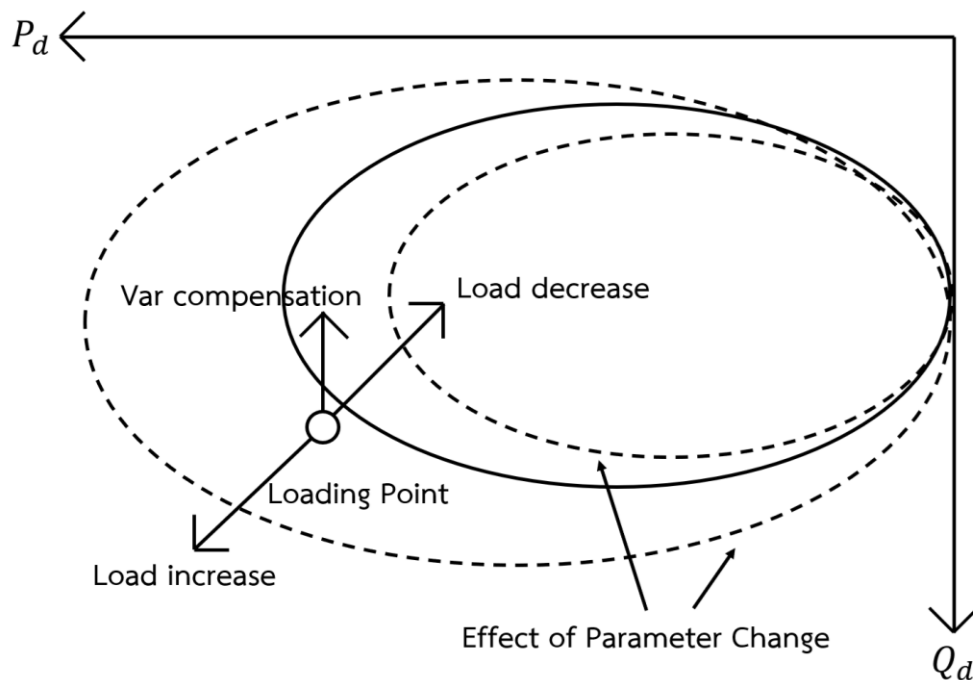
Figure 5.1 Effects of parameter changes to feasible region

5.2 Load shedding

Load shedding is power system operation. This operation will reduce less important load demand by setting off some load bus or load area. This method can reduce total load demand of the power system as a result loading point problem which is outside feasible region is solved by expanding the load security region in direction of load increment to cover that loading point. Though, load security region can be moved in direction of load increment. Loading points which are near 0 MW in some power system case cannot operate because generator minimum limit is higher than load demand.

Load shedding will operate automatically owning to the effectiveness. Moreover, load shedding will operate in unpredicted situations and must work regardless of where the system has split or whether communications are available. In addition, load shedding should avoid the possible tripping of certain lines because of overloading caused by changes in the load distribution. However, load shedding should be at widely and uniformly distributed points in the network.

5.3 PV installation

Nowadays, fossil fuels are steadily decreasing. In addition, Thailand has a high proportion of the dependence on natural gas from external energy sources. Several researches are found that there are often reports of natural gas supply problems through gas pipelines to Thailand or periodic reports of problems in the maintenance of natural gas fields in neighboring countries. Thus, causing the risk of electricity in the country coupled with the construction of a large power plant or a conventional power plants are difficult, which directly affects the construction of a new power plant. Hence, the government has a policy to promote electricity production from small power plants or distributed generation (DG) including renewable power plants, which tend to receive lower resistance from the public sector. Thereby, distributed generation (DG) is a key factor in the power system.

DG is treated as a generator in the power system as conventional generator within the customer side of the network or distribution networks. Thus, DG should be placed in the system close to the user of electric energy. DG has several benefits. DG can reduce power loss where DG is installed near the load bus. In addition, DG can improve power quality of the power system. Moreover, DG can reduce carbon emissions by using clean distributed generation, such as, PV and wind turbine. Additionally, DG can be classified into 4 types as follow.

1. Type 1: DG generating active power only, such as, fuel cells, photovoltaic.
2. Type 2: DG generating reactive power only, such as, capacitors, synchronous compensator etc.
3. Type 3: DG generating both active and reactive power, such as, synchronous machines.
4. Type 4: DG generating real but absorbing reactive power, such as, induction generators used in the wind turbines.

The DG can be integrated with the grid as presented in Figure 5.2. Nonetheless, DG is planned to be near the consumer load but determination of the location from point of common coupling (PCC) to the grid is key factor for the operation planner.
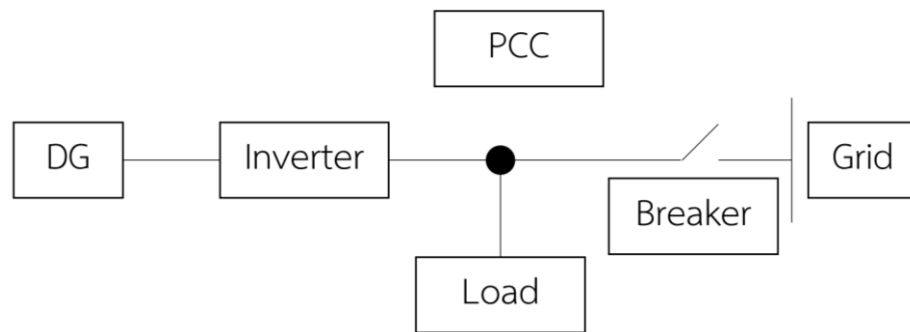

Figure 5.2 Schematic diagram of DG integration

Solar is a popular renewable energy used to generate electricity. Because there are many important advantages such as clean energy without pollution. Solar energy can be used cost-effectively and never run out. The process of generating electricity from solar cells does not emit carbon, so PV does not cause environmental pollution. In the past, Thailand has been continuously developing and promoting solar power generation for both types of solar PV farm and solar PV rooftop because of the geographical advantage of Thailand located in the equator. Thus, it has the potential of solar intensity high enough for power generation throughout the year. In addition, the government has continued to support solar energy.

Solar cells generate electrical energy by absorbing solar energy in the form of light intensity. Then converted solar energy to electrical energy in the form of direct current (DC). Solar cell cannot be connected to an electrical system or electrical appliances because electrical system applies only alternating current (AC) so solar cells must be connected through an inverter to convert DC power to AC power first.

This section will describe about PV impact to shape the load security region. The PV is treated as a generator which supplies active and reactive power to the power system where is installed near consumer load. The load security region will be expanded because total generator capacity of the power system is increased. However, the load security region can be moved along the direction of load increment. The movement of load security region cause that the minimum active power limit is increased as shown in Figure 5.1. The minimum active power limit of load security region is moved owing to minimum total generator limit which is increased from PV installation in the power system. From the above, the PV is a key factor to solve load demand expansion problem in the power system.

CHAPTER 6

Numerical Results

This chapter presents the numerical results of test on the power system. The results are illustrated on the P-Q plane by using tracing algorithm. The P-Q plane includes 2 parts where x-axis is active power demand and y-axis is reactive power demand. The first part is prediction point set. This part is generated by prediction process. The second part is load security region which is the power flow solution set on the boundary. These solution set are obtained by optimization-based method.

6.1 Base Case of the Power System

This section considers only the base case of the power systems. Base case is the test case without modifying the power system parameter and adding any device. Six-bus system and nine-bus system are tested in this section. This work chooses six-bus system and nine-bus system to represent as small size and non-complex power system although these power systems are such similar. The purpose is to show the different of tracing algorithm parameter changing. The tracing algorithm parameter changing includes step size and first prediction point.

6.1.1 Six-Bus System

The six-bus system is demonstrated in the appendix A.1 from [34]. These implements are set into 3 cases. The first case defined load bus 4 as sink bus. The second case defined load bus 5 as sink bus. The last case defined load bus 6 as sink bus. In addition, all generator buses are defined as source bus in each case. Sink bus is an objective load bus parameter which is set as a variable instead of constant. The other load buses remain unchanged and is set as constant load demand. Besides, the source bus is generator bus variables.

From case with the objective load bus at 4, load security region is visualized as shown in Figure 6.1. In this case, the first prediction point is -150j MVA and step size is 15 MVA. The total of iterations is 89 rounds and computation time is 80.99 seconds. The solid line is the load security region. Besides, the dash line is the prediction point set from prediction process.
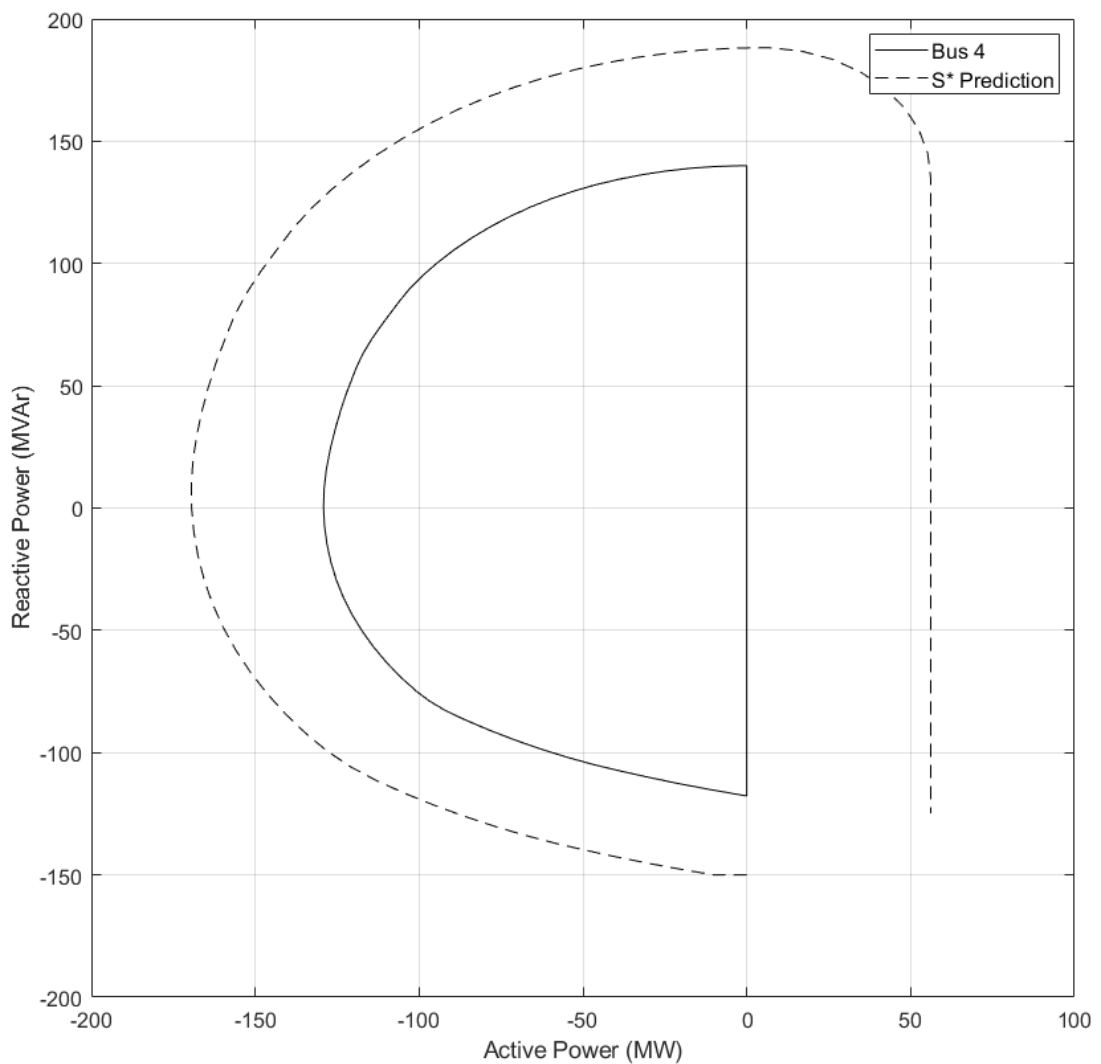

Figure 6.1 Load security region (Source: All generator / Sink: Bus 4)

From case with the objective load bus at 5, load security region is visualized as shown in Figure 6.2. In this case, the first prediction point is -150j MVA and step size is 15 MVA. The total of iterations is 103 rounds and computation time is 94.40 seconds. Besides, the dash line is the prediction point set from prediction process.
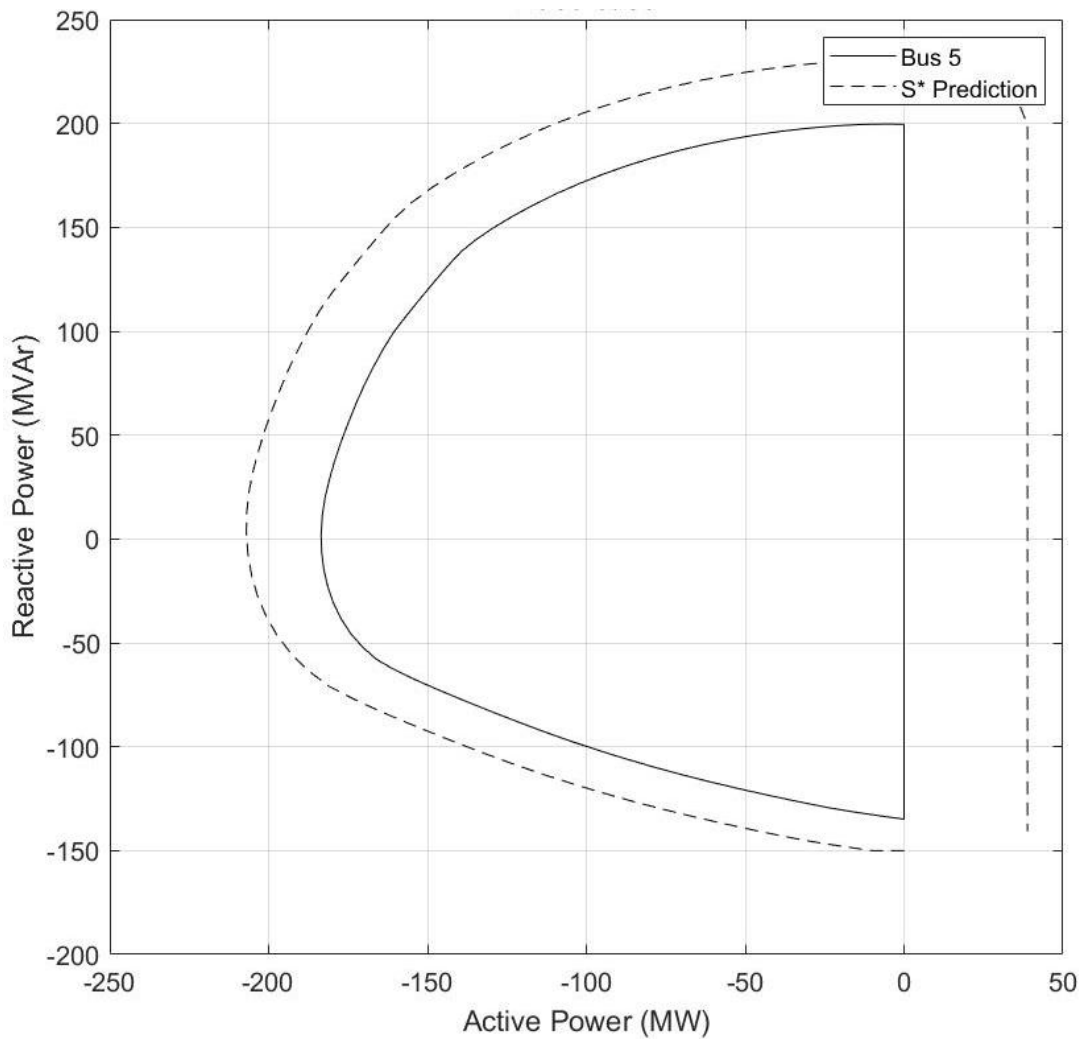

Figure 6.2 Load security region (Source: All generator / Sink: Bus 5)

From case with the objective load bus at 6, load security region is visualized as shown in Figure 6.3. In this case, the first prediction point is -150j MVA and step size is 15 MVA. The total of iterations is 108 rounds and computation time is 101.06 seconds. Besides, the dash line is the prediction point set from prediction process.
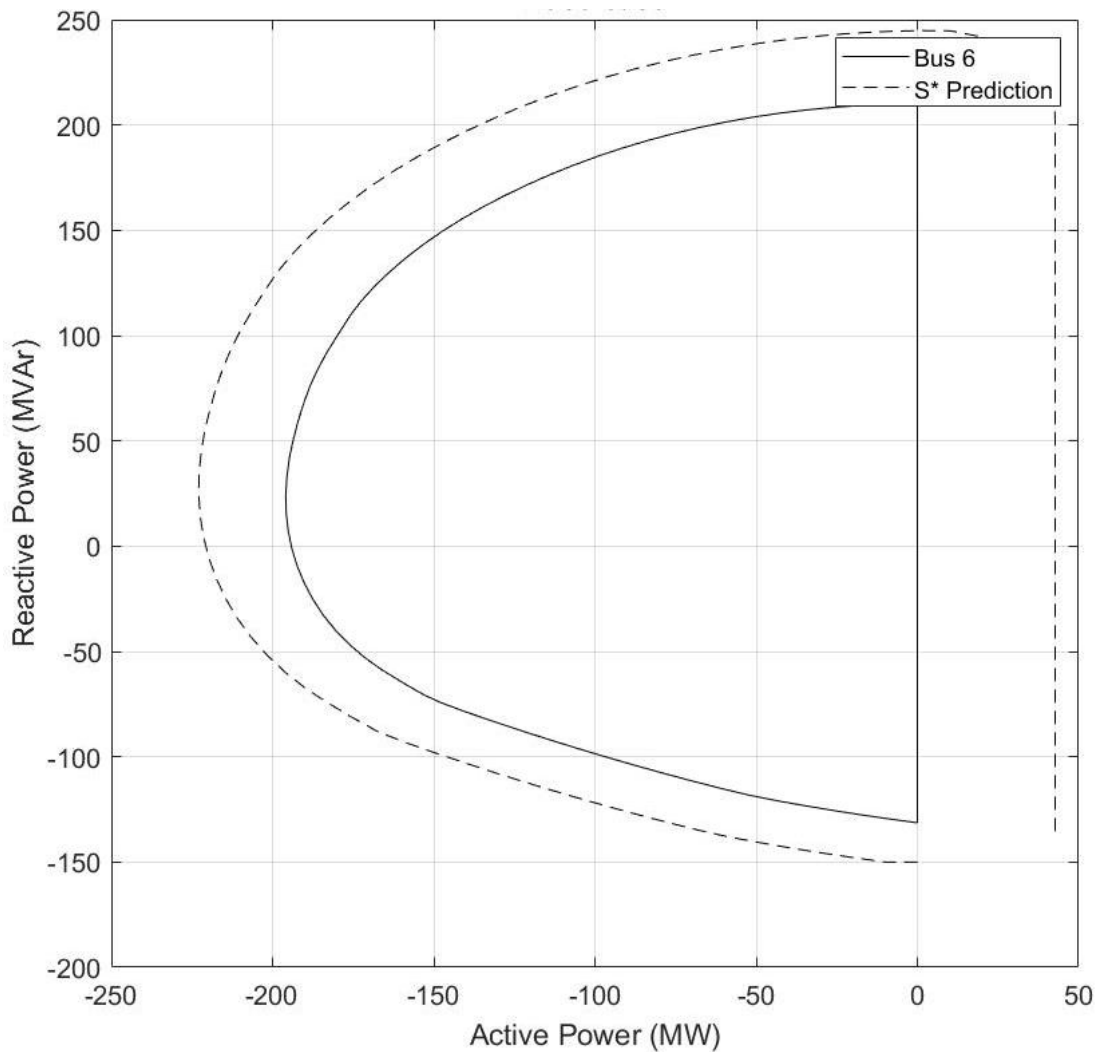

Figure 6.3 Load security region (Source: All generator / Sink: Bus 6)

The load security region of all cases is assembled in Figure 6.4. The solid line is sink bus at bus 4. The dash line is sink bus at bus 5. The dash-dot line is sink bus at bus 6.
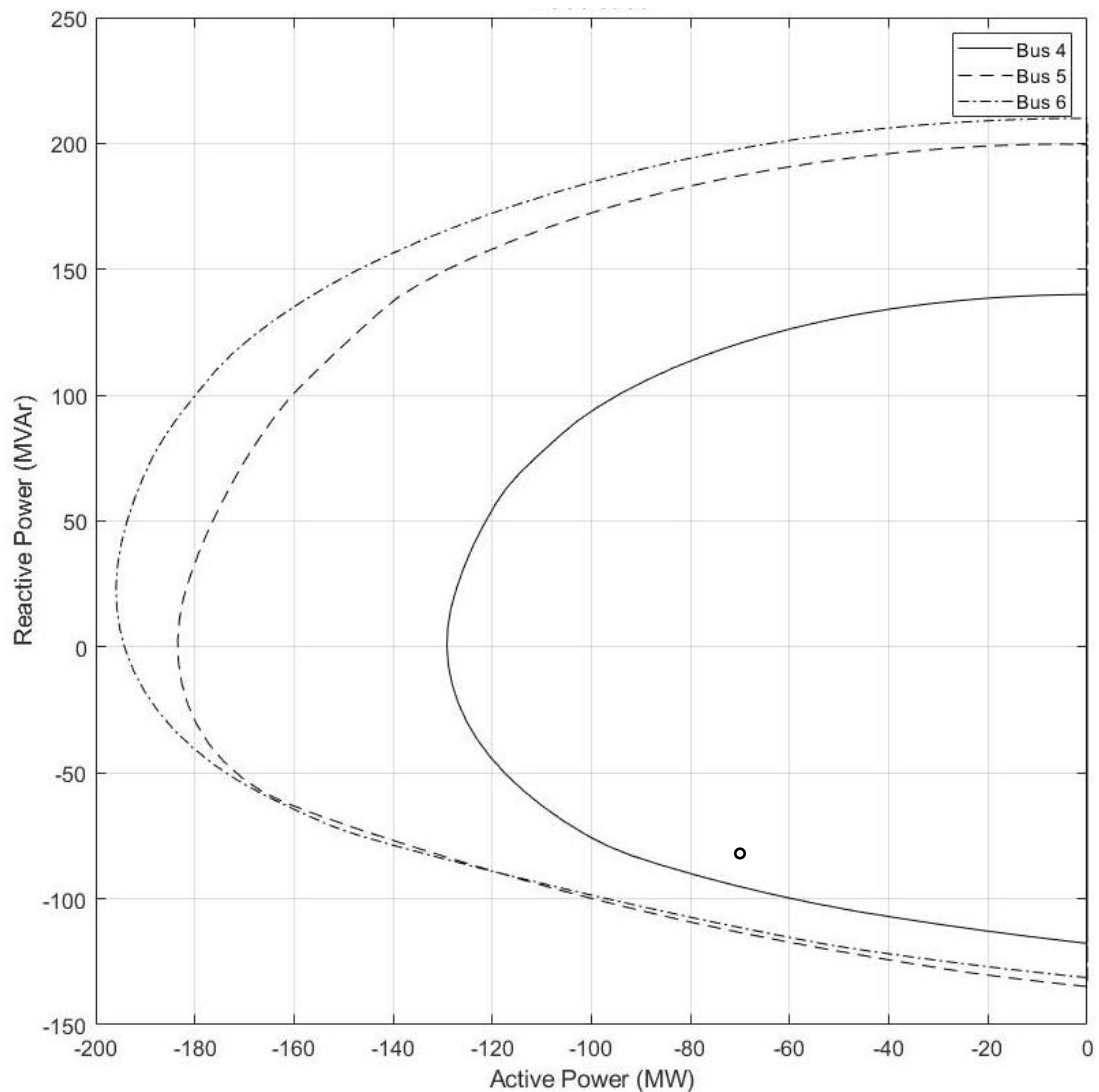
Figure 6.4 Load security region (Source: All generator / Sink: Bus 4,5, and 6)

6.1.2 Nine-Bus System

The nine-bus system is demonstrated in the appendix A.2 from [35]. These implements are set into 3 cases. The first case defined load bus 5 as sink bus. The second case defined load bus 7 as sink bus. The last case defined load bus 9 as sink bus. In addition, all generator buses are defined as source bus in each case. Sink bus is an objective load bus parameter which is set as a variable instead of constant. The other load buses remain unchanged and is set as constant load demand. Besides, the source bus is generator bus variables.

From case with the objective load bus at 5, load security region is visualized as shown in Figure 6.5. In this case, the first prediction point is -300j MVA and step size is 30 MVA. The total of iterations is 76 rounds and computation time is 56.80 seconds. Besides, the dash line is the prediction point set from prediction process.

Figure 6.5 Load security region (Source: All generator / Sink: Bus 5)

From case with the objective load bus at 7, load security region is visualized as shown in Figure 6.6. In this case, the first prediction point is -300j MVA and step size is 30 MVA. The total of iterations is 71 rounds and computation time is 49.9154 seconds. Besides, the dash line is the prediction point set from prediction process.
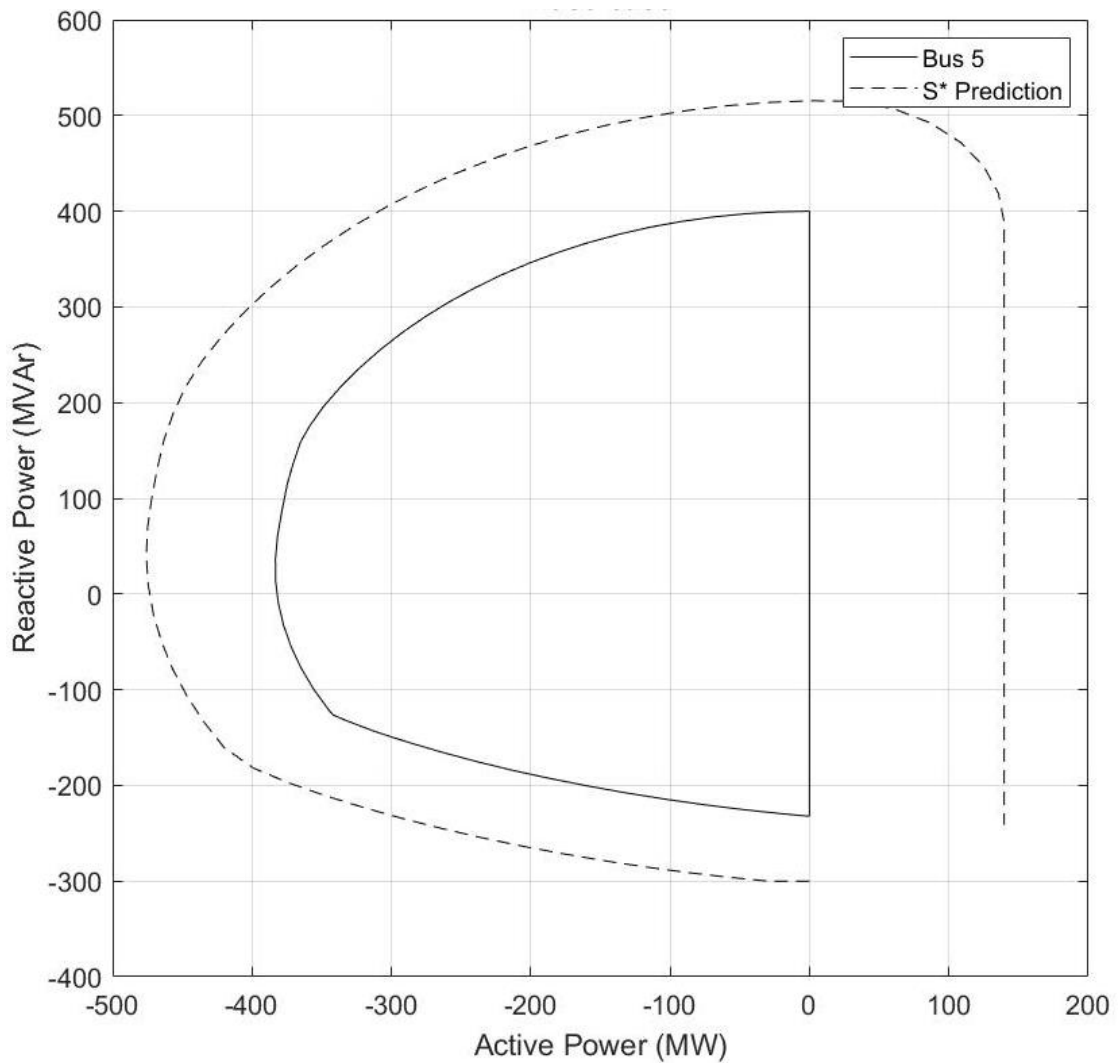

Figure 6.6 Load security region (Source: All generator / Sink: Bus 7)

From case with the objective load bus at 9, load security region is visualized as shown in Figure 6.7. In this case, the first prediction point is -300j MVA and step size is 30 MVA. The total of iterations is 85 rounds and computation time is 60.11 seconds. Besides, the dash line is the prediction point set from prediction process.
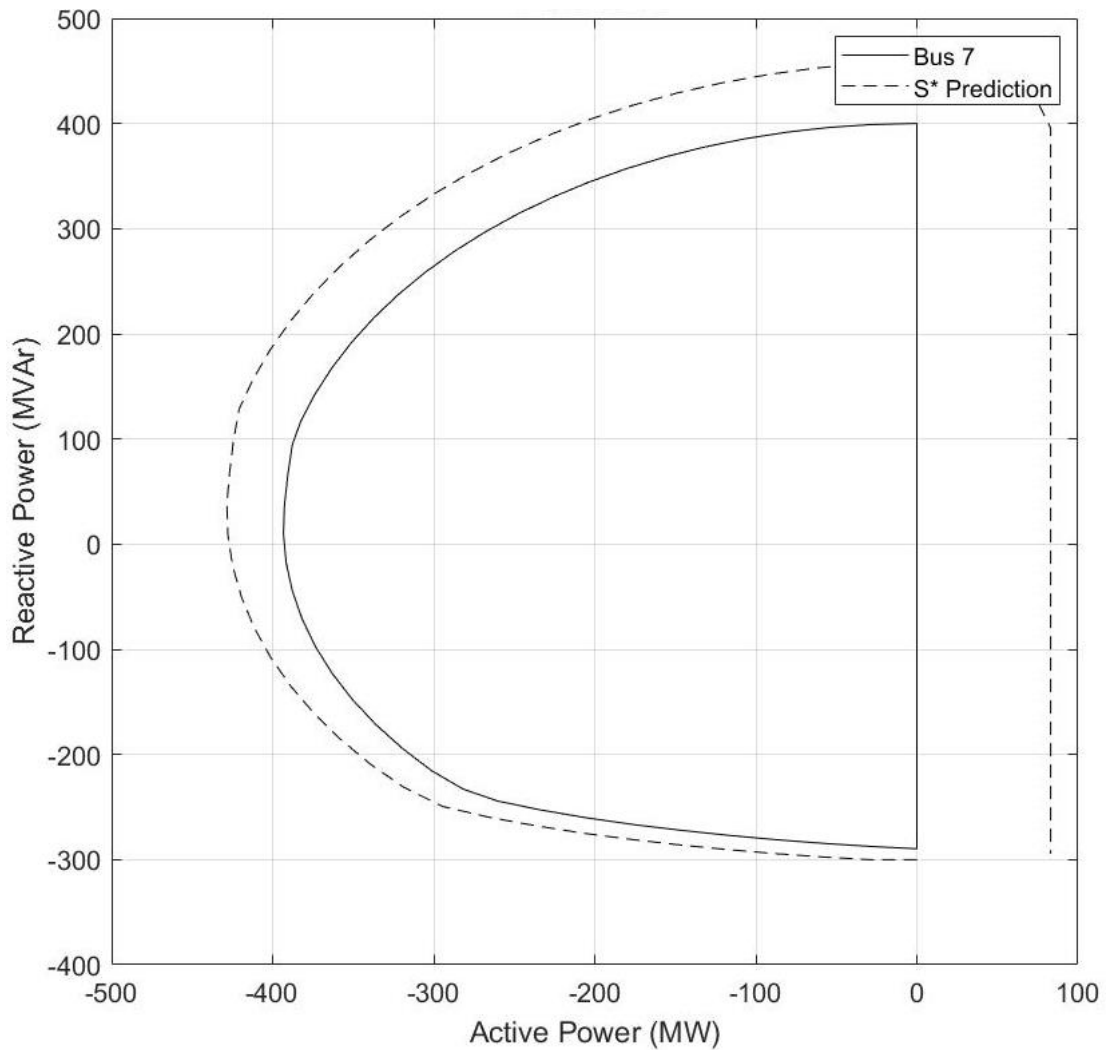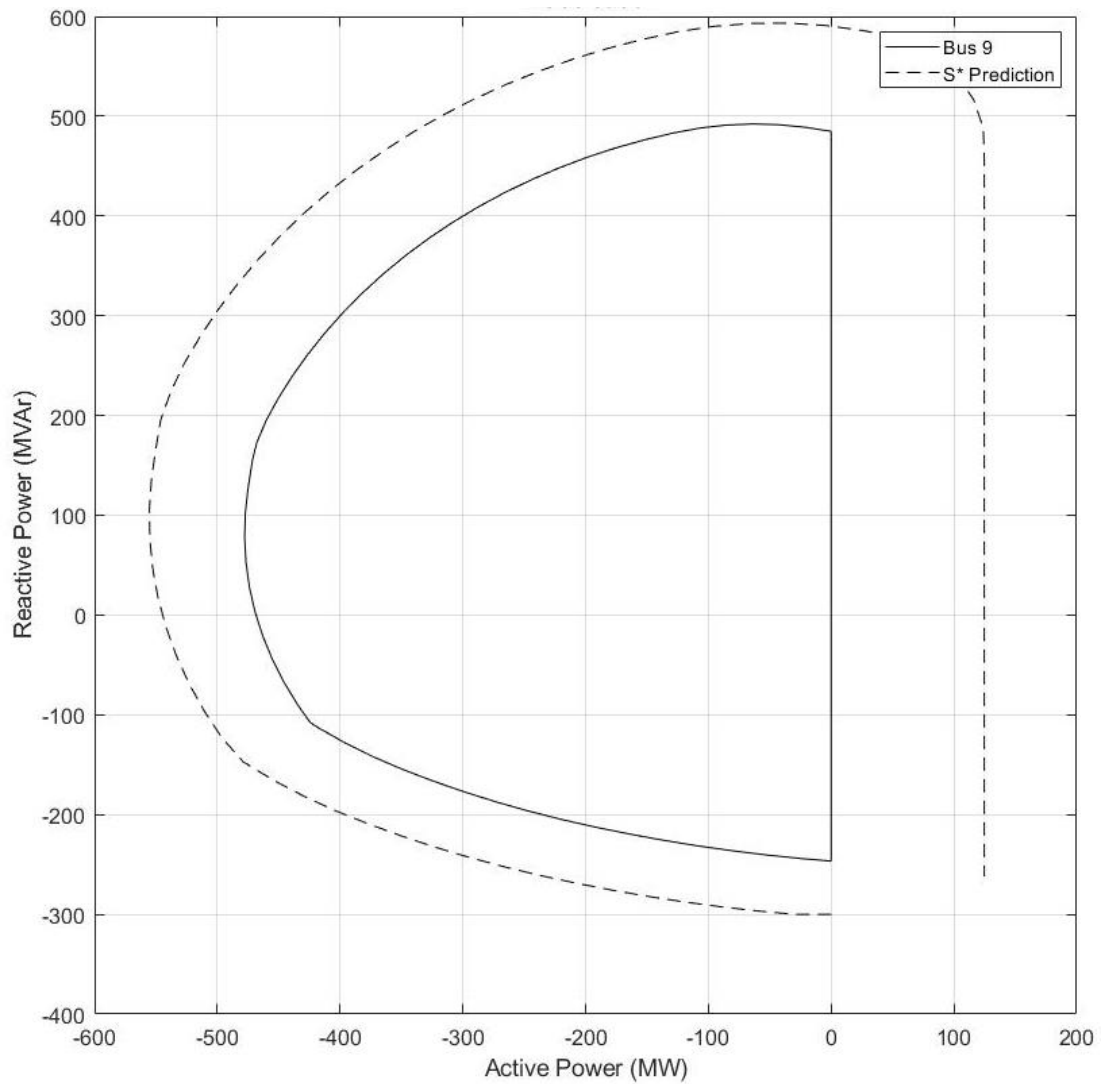

Figure 6.7 Load security region (Source: All generator / Sink: Bus 9)

The load security region of all cases is assembled in Figure 6.8. The solid line is sink bus at bus 5. The dash line is sink bus at bus 7. The dash-dot line is sink bus at bus 9.
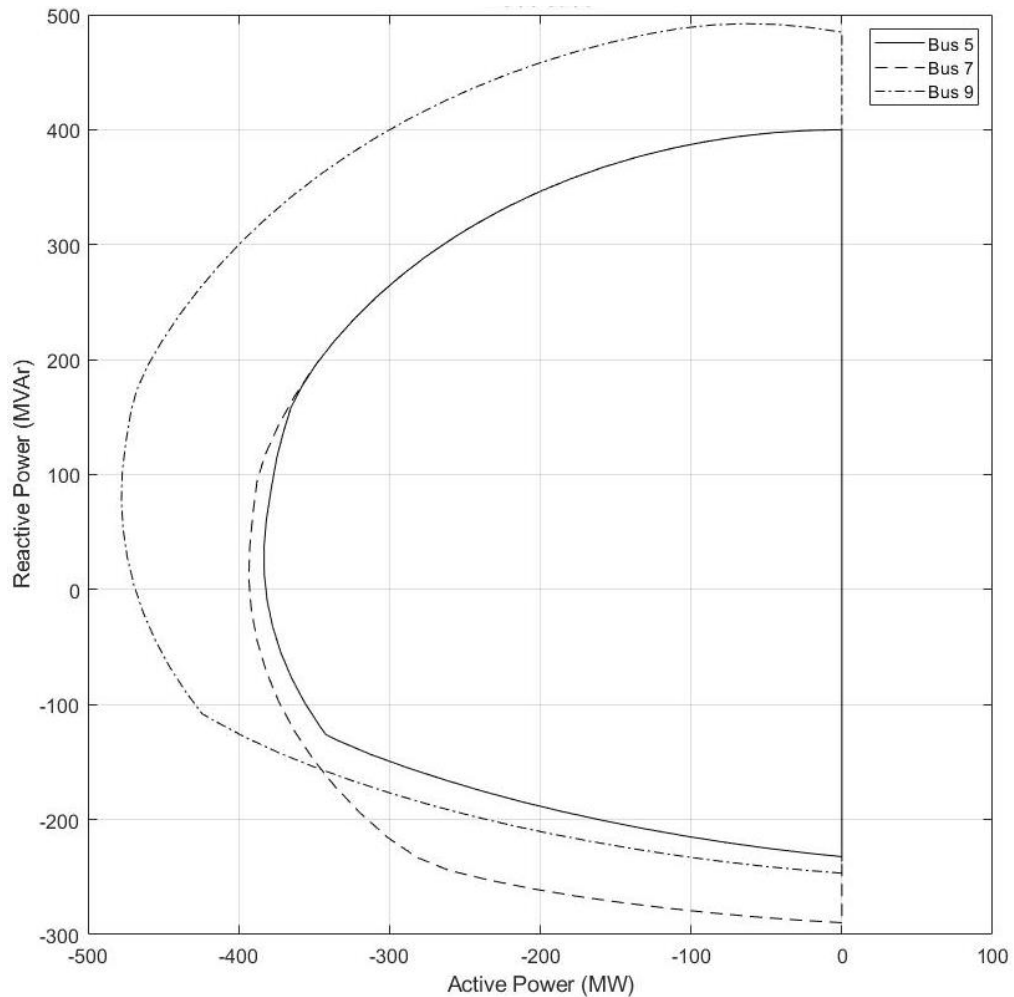
Figure 6.8 Load security region (Source: All generator / Sink: Bus 5,7, and 9)

6.2 Area to area

This section determines load security region from source area to sink area. Source area is considered by all generator bus in the power system. Sink area is considered by all load bus in attentive area. In additionally, the objective of this section is to obtain the maximum load security region which can operate by using not only single load bus but also all load buses. However, sink area does not necessary to include all load bus in the power system.

This test comprises 3 power system tests as follows six-bus system, nine-bus system, and 24-bus system. This work considers six-bus and nine-bus system as small scale and non-complex power system for comparing between base case and area to area. In addition, this work considers 24-bus system as large scale and complex power system because this system includes 4 areas.

6.2.1 Six-Bus System

The six-bus system is demonstrated in the appendix A.1 from [34]. This implement sets all generator buses which are bus 1, 2, and 3 as source area and sets all load buses which are bus 4, 5, and 6 as sink area. In the other words, this test sets generator and load buses as variable.

The first prediction point of this test is -150j MVA and step size is 30 MVA. The total of iterations is 88 rounds and computation time is 63.07 seconds. Besides, the dash line is the prediction point set from prediction process. Figure 6.9 shows load security region of 6-bus system form all generator to all load bus. Moreover, this figure show that load security region is larger than determine single sink bus.

Figure 6.9 Load security region (Source: All generator / Sink: All load bus)

6.2.2 Nine-Bus System

The nine-bus system is demonstrated in the appendix A.2. This implement sets all generator buses which are bus 1, 2, and 3 as source area and sets all load buses which are bus 5, 7, and 9 as sink area. Bus 4, 6, and 8 are installed transformer. For this reason, this test does not include these buses to sink area. In summary, this test transfers power from source area (bus 1, 2, and 3) to sink area (bus 5, 7, and 9).

The first prediction point of this test is -300j MVA and step size is 60 MVA. The total of iterations is 106 rounds and computation time is 67.27 seconds. Besides, the dash line is the prediction point set from prediction process. Figure 6.10 show that load security region is larger than determine single sink bus.
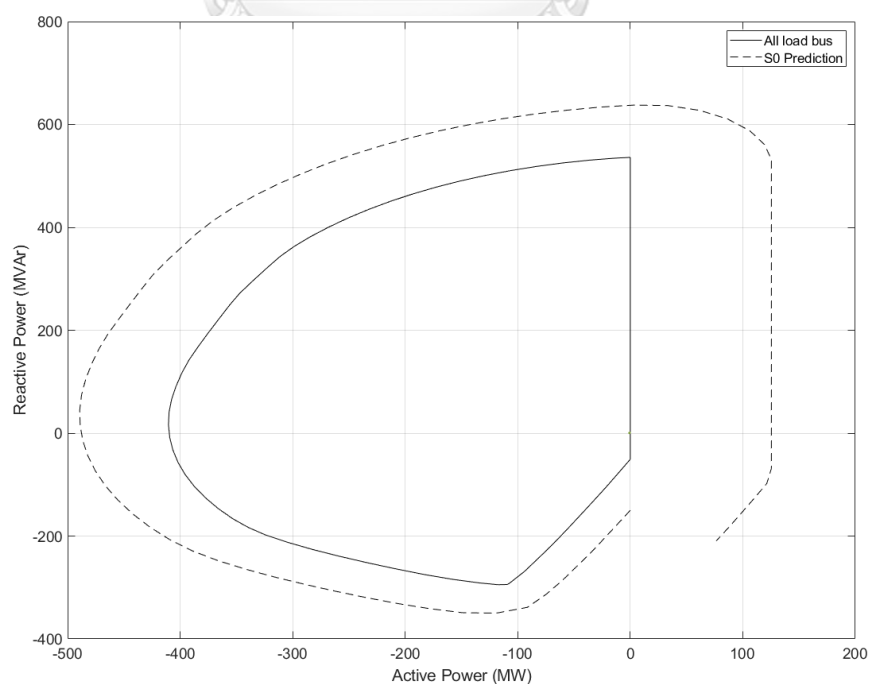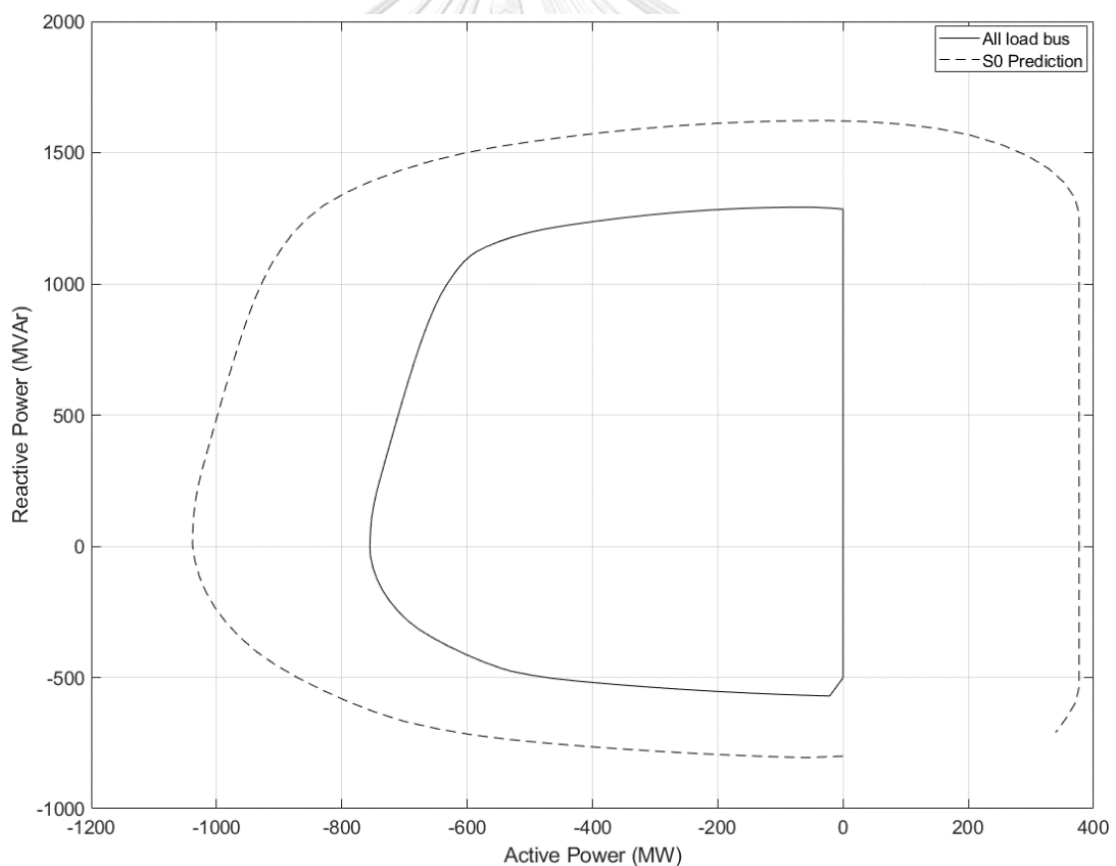

Figure 6.10 Load security region (Source: All generator / Sink: Bus 5,7, and 9)

6.2.3 24-Bus System

The 24-bus system is demonstrated in the appendix A.3 from [37]. This system comprises 33 generations, 17 load buses, and 4 areas. The implementations are set into 4 test cases as follow the 4 areas. Area 1 consists of bus 1-5 and 9. Area 2 consists of bus 6-8 and 10. Area 3 consists of bus 11-14, 19-20 and 23. Area 4 consists of bus 15-18, 21-22 and 24. However, this system is so complicated because some PV bus has load demand. In summary, these implementations set all generators are set as source area and. Additionally, these implementations set all PQ buses as sink area and set all PV buses which has load demand in that bus as shown in Table 6.1.

Table 6.1 Sink bus of each area

Sink area	Sink bus
1	1,2,3,4,5,9
2	6,7,8,10
3	13,14,19,20
4	15,16,18

Load security region of sink area 1 is shown in Figure 6.11. The first prediction point of this test is -800j MVA and step size is 60 MVA. The total of iterations is 169 rounds and computation time is 267.15 seconds.

Figure 6.11 Load security region (Source: All generator / Sink area: 1)

Load security region of sink area 2 is shown in Figure 6.12. The first prediction point of this test is -800j MVA and step size is 60 MVA. The total of iterations is 133 rounds and computation time is 206.27 seconds.
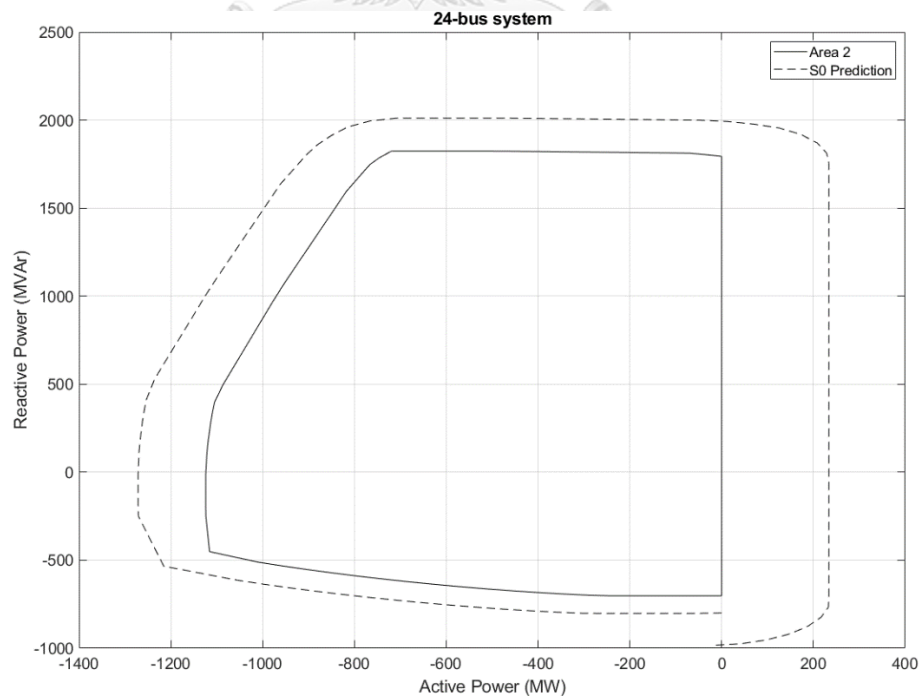
Figure 6.12 Load security region (Source: All generator / Sink area: 2)

Load security region of sink area 3 is shown in Figure 6.13. The first prediction point of this test is -800j MVA and step size is 60 MVA. The total of iterations is 277 rounds and computation time is 463.71 seconds.
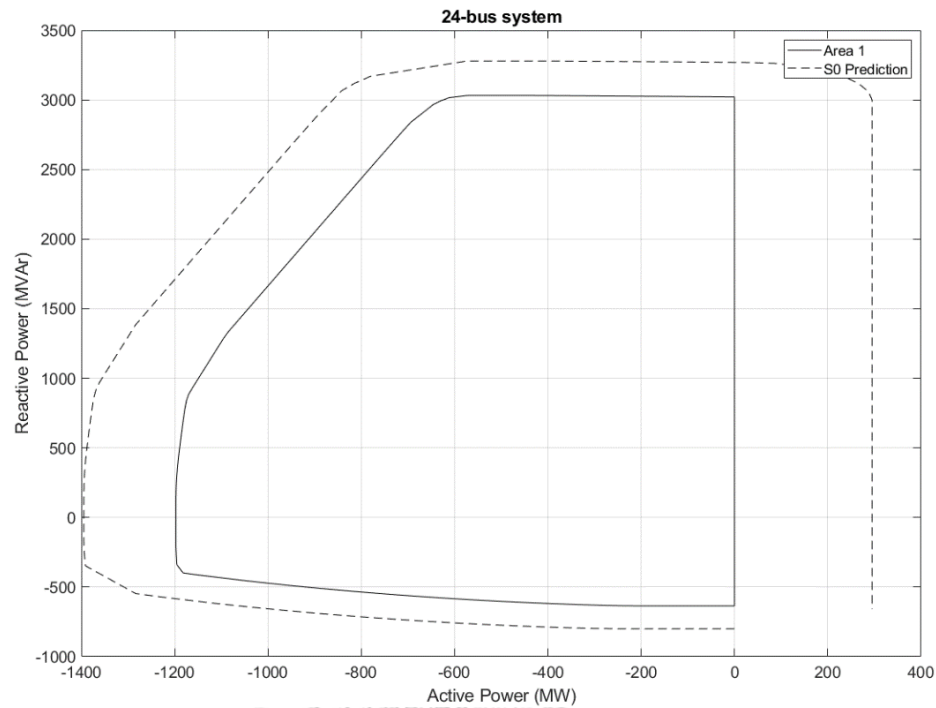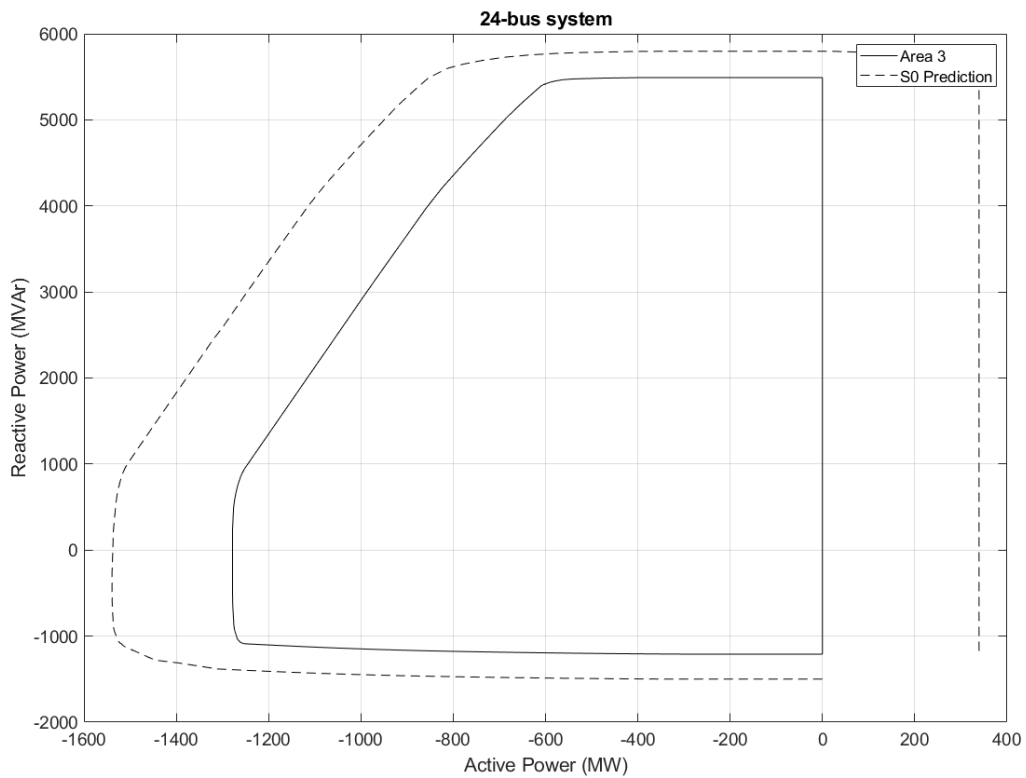

Figure 6.13 Load security region (Source: All generator / Sink area: 3)

Load security region of sink area 4 is shown in Figure 6.14. The first prediction point of this test is -800j MVA and step size is 60 MVA. The total of iterations is 286 rounds and computation time is 454.25 seconds.
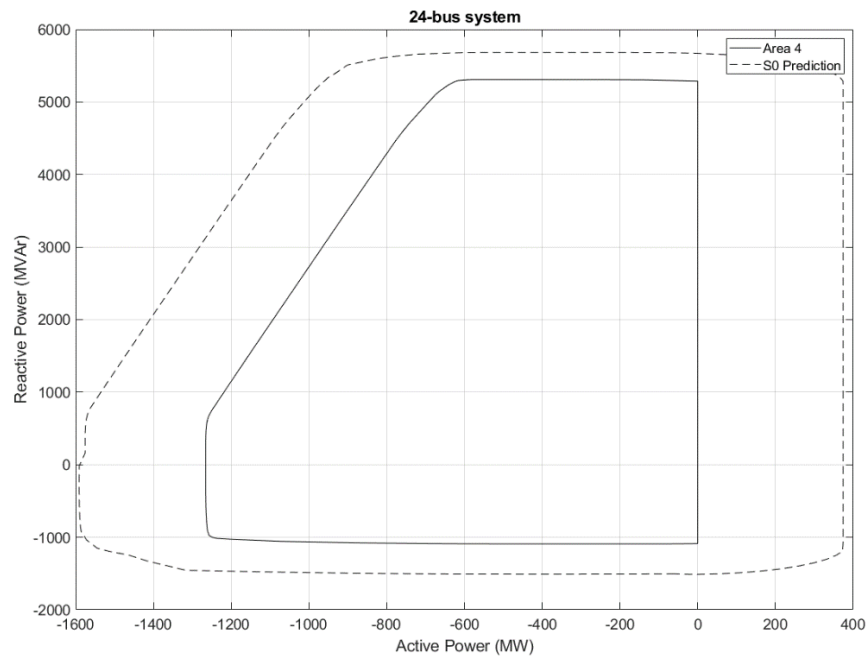
Figure 6.14 Load security region (Source: All generator / Sink area: 4)

The load security regions of all cases are assembled in Figure 6.15. The solid line is sink area 1. The dash line is sink area 2. The dotted line is sink area 3. The dash-dot line is sink area 4.
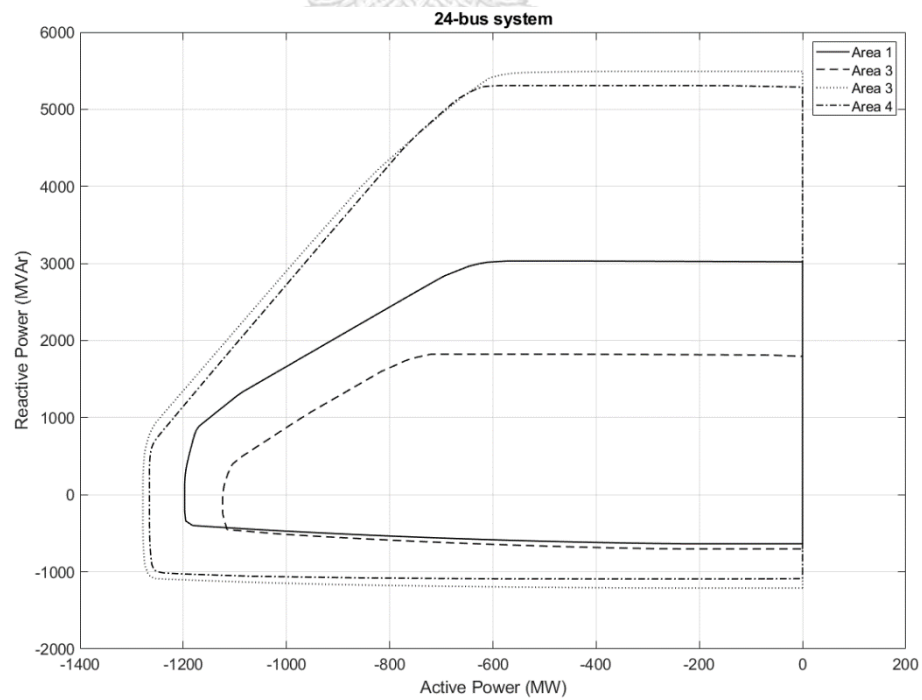
Figure 6.15 Load security region (Source: All generator / Sink area: 1,2,3, and 4)

6.3 Load Shedding

Load shedding is implemented in this section. The implementations consider six-bus system and shed load. Furthermore, this implementation determines load bus 4, 5, and 6 as sink bus for each case. Then, this test sheds other load bus to examine load security region variation. When load shedding at bus 4, the total load at bus 4 is set to 0 MVA and another load bus remains unchanged as base load. Moreover, sink bus still be set as variable.

From sink bus 4 with load shedding other bus, load security region is visualized as shown in Figure 6.16. In this case, the first prediction point is -150j MVA and step size is 15 MVA. Besides, the solid line is base case. The dotted line is load shedding at bus 5. The dashed line is load shedding at bus 6. The circle is base loading point.

Figure 6.16 Load security region of load bus 4 with load shedding

From sink bus 5 with load shedding other bus, load security region is visualized as shown in Figure 6.17. In this case, the first prediction point is -150j MVA and step size is 15 MVA. Besides, the solid line is base case. The dotted line is load shedding at bus 4. The dashed line is load shedding at bus 6. The circle is base loading point.
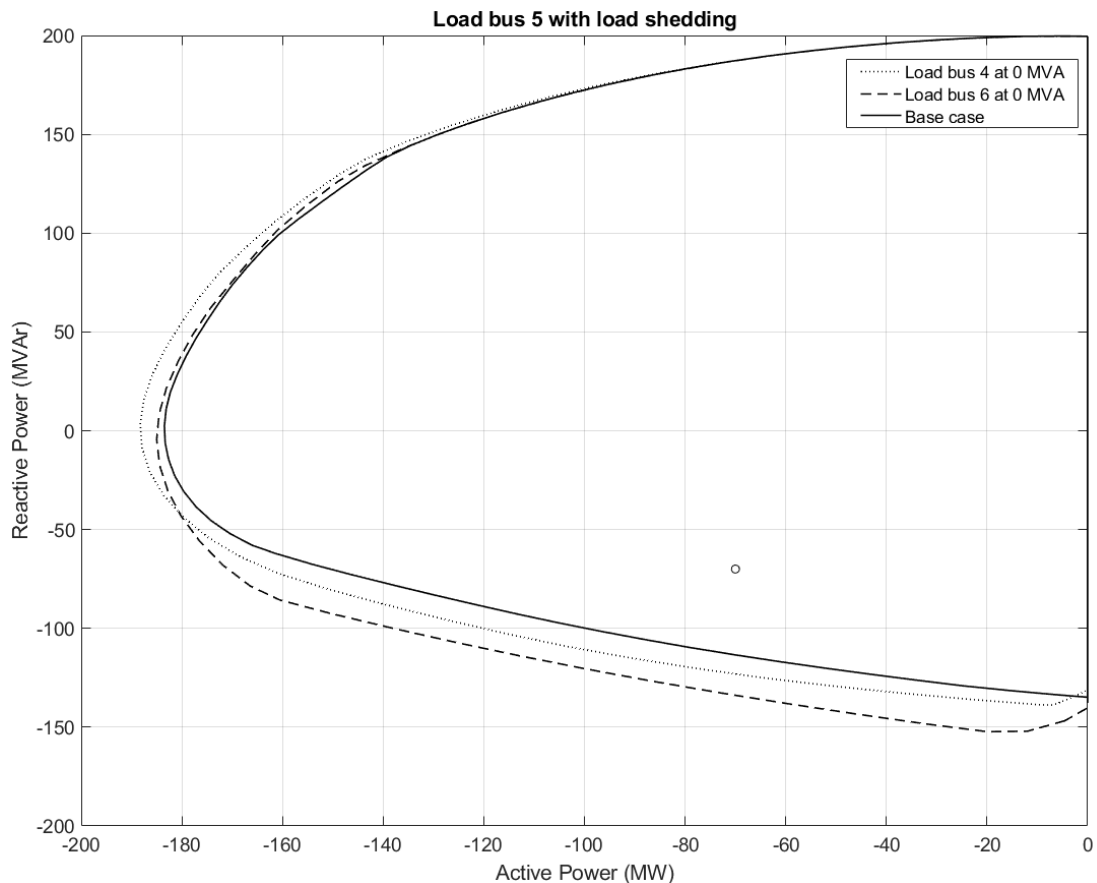
Figure 6.17 Load security region of load bus 5 with load shedding

From sink bus 6 with load shedding other bus, load security region is visualized as shown in Figure 6.18. In this case, the first prediction point is -150j MVA and step size is 15 MVA. Besides, the solid line is base case. The dotted line is load shedding at bus 4. The dashed line is load shedding at bus 5. The circle is base loading point.
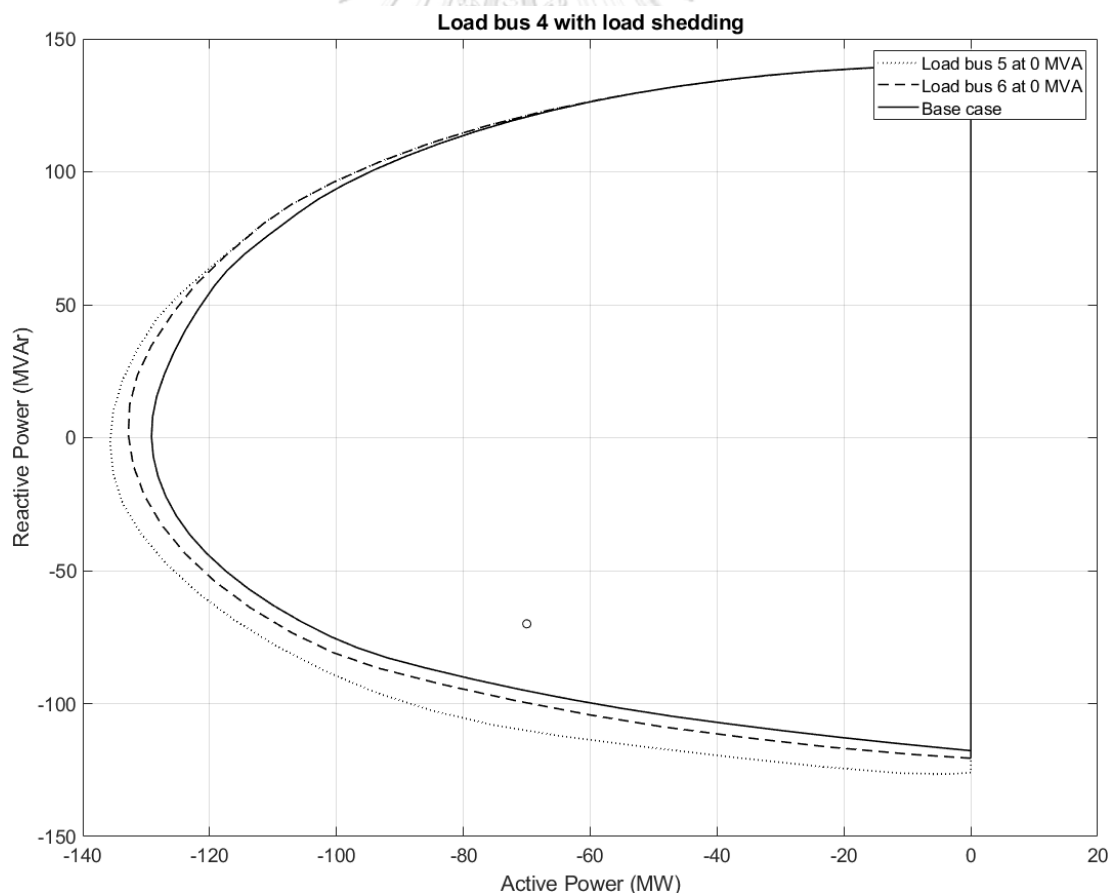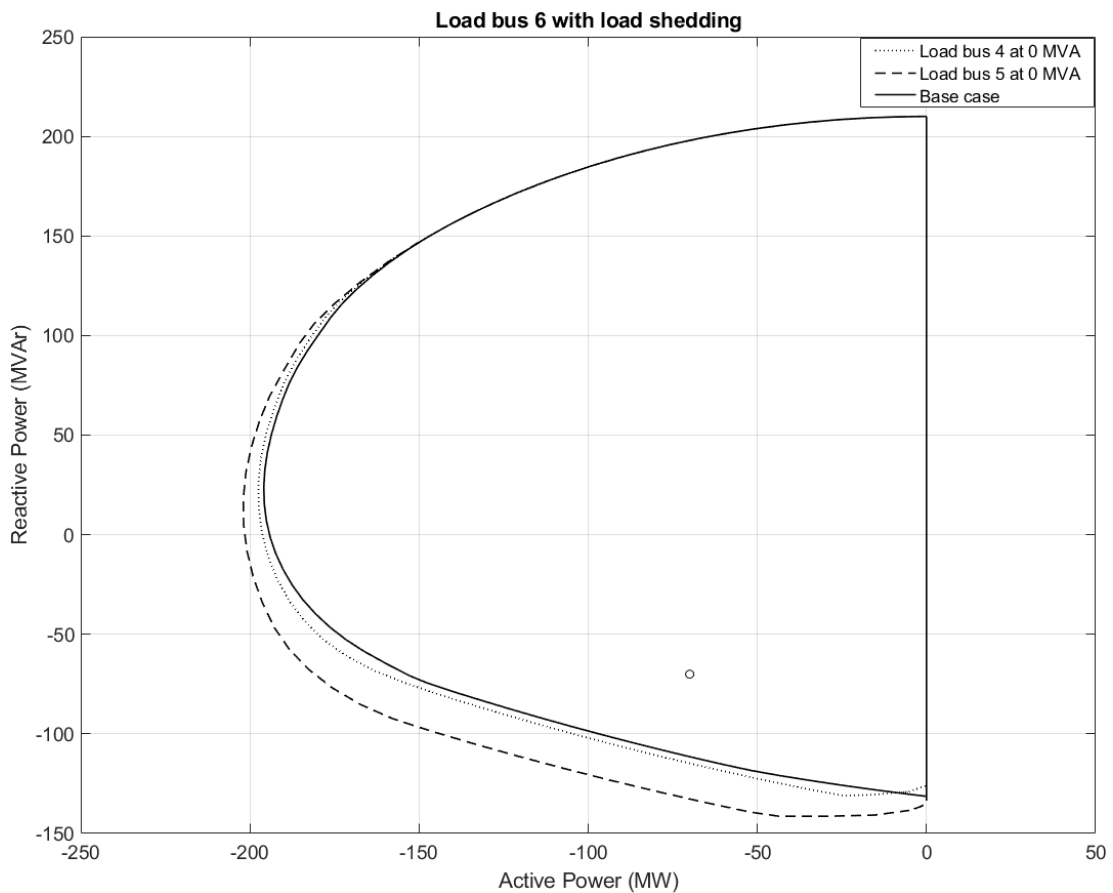
Figure 6.18 Load security region of load bus 6 with load shedding

6.4 Installing PV system

Solar cell is installed in this section. This device is used as a new generation in the test system. The implementations also consider all generator bus as source bus and consider each load buses as sink bus in six-bus system. Besides, the solar cell is installed only in bus 4. The objective of this test is to determine the impact of solar cell for each sink bus. The implementations includes 4 cases. This work determines load security region for load bus 4, 5, 6, and all load buses.

From Figure 6.19, load bus 4 is set as sink bus and installed solar cell in this bus. This test treats all generator buses as source bus. First prediction point is set to -250 j MVA and step size is set to 15 MVA. The total of iterations is 93 rounds and computation time is 73.59 seconds.

From Figure 6.20, load bus 5 is set as sink bus and installed solar cell in bus 4. This test treats all generator buses as source bus. First prediction point is set to -250 j MVA and step size is set to 15 MVA. The total of iterations is 102 rounds and computation time is 71.04 seconds.

From Figure 6.21, load bus 5 is set as sink bus and installed solar cell in bus 4. This test treats all generator buses as source bus. First prediction point is set to -250 j MVA and step size is set to 15 MVA. The total of iterations is 105 rounds and computation time is 72.80 seconds.

From Figure 6.22, load bus 4, 5, and 6 are set as sink area and installed solar cell in bus 4. This test treats all generator buses as source bus. First prediction point is set to -250j MVA and step size is set to 15 MVA. The total of iterations is 182 rounds and computation time is 130.45 seconds.
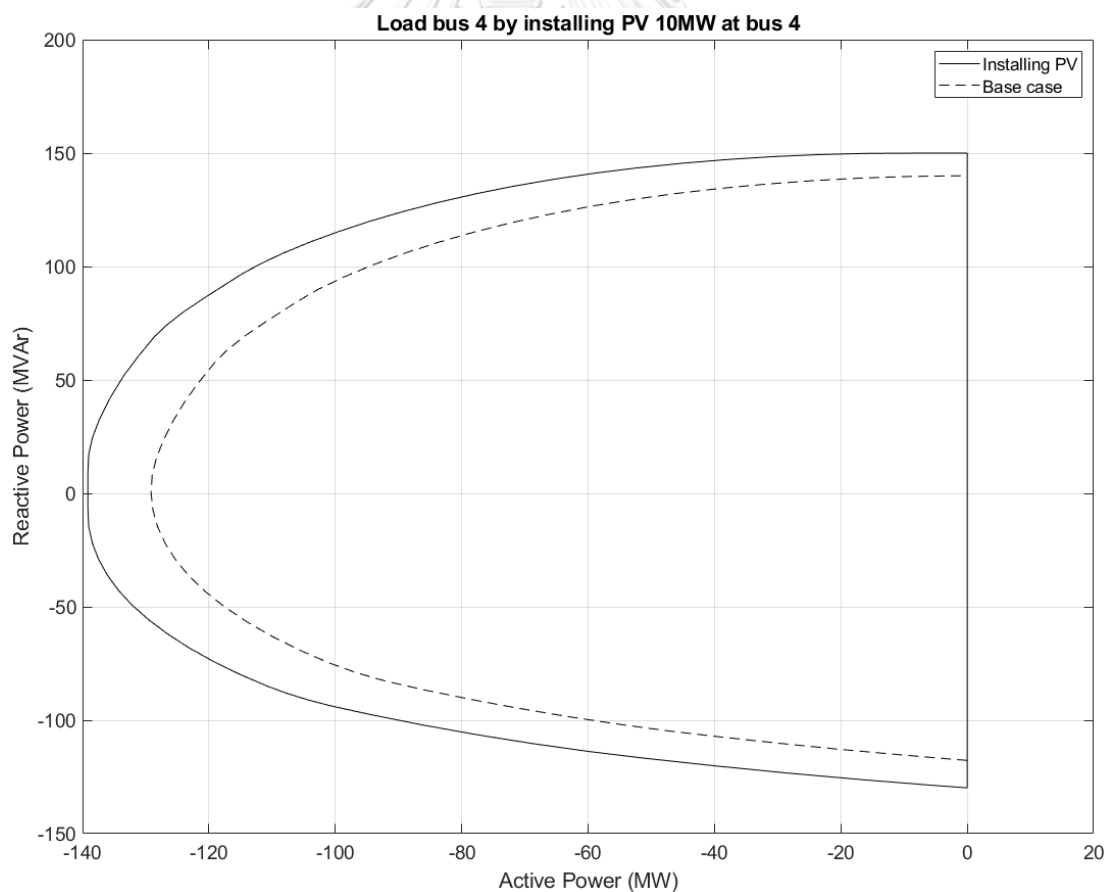
Figure 6.19 Load security region of load bus 4 with PV installing
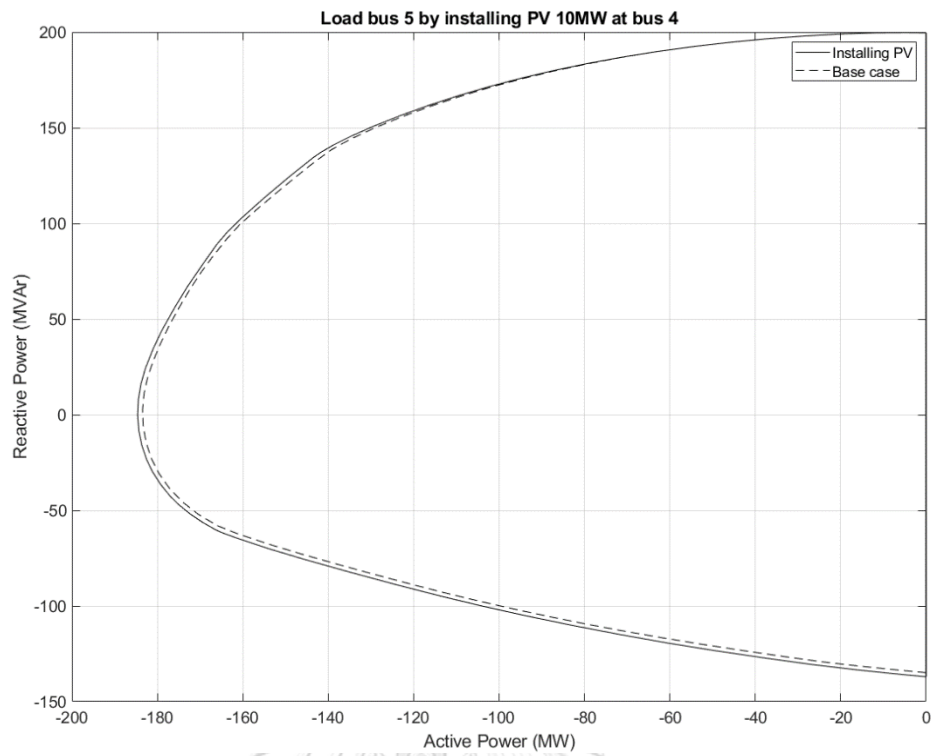
Figure 6.20 Load security region of load bus 5 with PV installing
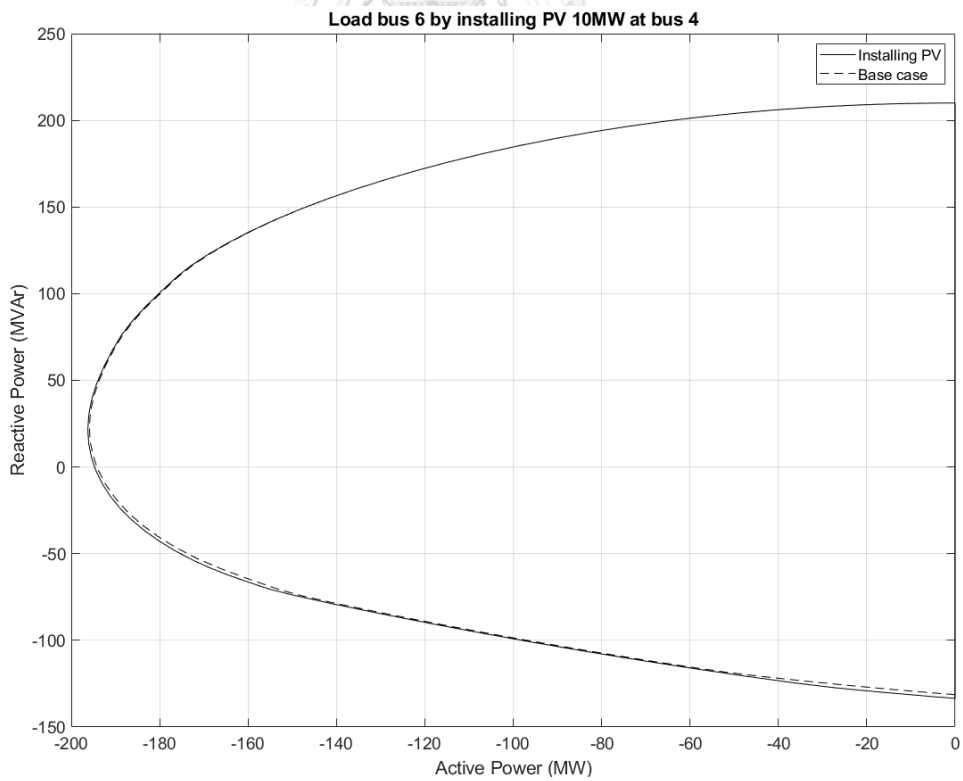
Figure 6.21 Load security region of load bus 6 with PV installing
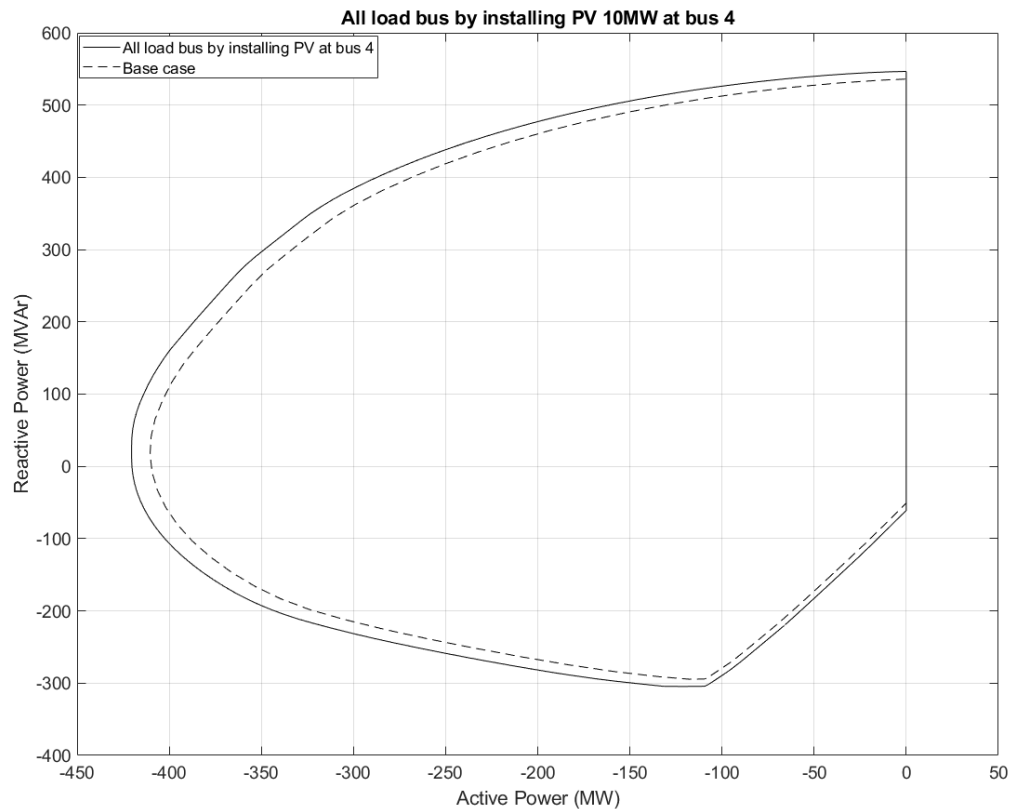
Figure 6.22 Load security region of sink area with PV installing

6.5 Summary

This section summarizes the numerical results of this work. This summary consists of 4 parts. First part is power transfer from all generators to a single load bus for base case of six-bus and nine-bus system. Second part is power transfer from all source areas to a sink area for base case of six-bus, nine-bus, and 24-bus system. Last but not least, third part is a modified case from the first part by load shedding for six-bus system. Last part is a modified case from the first part as the third part by installing PV for six-bus system.

The first part shows the load security region from 3 cases of six-bus system and 3 cases of nine-bus system. This implementation shows that each load bus of each system can be increased until reach the power system limit. The loading point can move within the load security region in every direction. From Figure 6.4, load security region of each load bus can be enlarged from base load 70 MW and 70 MVAr.

Moreover, this simulation can be used to find the weakest bus by measuring the radius from the base load toward the margin of the load security region. This radius circle must not exceed the load security region margin. The shortest radius bus is the weakest bus. In six-bus system, load bus 4 is the weakest bus. On the other hand, loading point in the load security region is the feasible point which does not violate the power system limit.

The second part shows the load security region from a case of six-bus system, cases of nine-bus system, and 4 cases of 24-bus system. This implementation shows that each sink area of each system can be increased until reach the power system limit. The sink buses of the first part are integrated into sink area. For this reason, load security region of six-bus and nine-bus system is larger than the load security region from the first part. In case 24-bus system, this test shows that the load security regions of area 3 and area 4 is larger than the load security regions of area 1 and area 2. Additionally, the area to area simulation is used to determine the total load of the whole power system. The margin point of the load security region contains each load bus data which can be plotted into sub load security region for each load bus. The sub security region describes the maximum load of each load bus. The number of sub security regions depends on the number of load buses in the power system. Thus, power system operator can use this load bus data set for planning the additional load in the future or setting the load limit constraints.

The third part shows the load security region from 3 cases of six-bus system. This implementation shows that each load bus of the system can be increased with load shedding until reach the power system limit. Due to load shedding, the load security region can be expanded or moved along the load incremental direction by decreasing load demand from another load bus and increasing to sink bus. However, size of the load security region can be shrunk because total generation must support total load demand with including power loss and produce power more than minimum limit. Thus, the load security region can be move along the load incremental direction

by load shedding, but the load security region can be shrunk owning to generation minimum limit and can be expanded where the generation minimum limit has no effect to the total load demand. In summary, this work suggests that the power system operator should shed load bus 5 first because load security regions are the largest after shedding load. Then, the power system operator should shed load bus 4 for maximizing active power demand or load bus 6 for maximizing load security region.

The last part shows the load security region from 4 cases of six-bus system. This implementation shows that each load bus of system can be increased with PV installing until reach the power system limit. The PV system which size is 10 MW and 10 MVAr is installed at bus 4. The PV is treated as a new generator bus. From load bus 4, the load security region is expanded by 10 MW and 10 MVAr because of PV size. From load bus 5 and bus 6, the load security region is slightly expanded where these load buses is not installed the PV. The load security region of load bus which is not installed the PV will be slightly expanded because the PV cannot transfer total power to this load bus due to the original power system constraints. Figure 6.22 shows that the load security region near 0 MW is shrunk. Nevertheless, power system operator should apply unit commitment to turn off some power generator for avoiding minimum generation limit during low load consumption to enlarge load security region.

CHAPTER 7

Conclusion and Future Work

This research proposes tracing algorithm with second order cone program (SOCP) relaxation to visualize load security region. This chapter predicates the concept of tracing algorithm and the proposed method with the test cases from chapter 6. Furthermore, this chapter provides the future work of this problem.

7.1 Conclusion

To illustrate load security region, this work proposes tracing algorithm with SOCP relaxation. This work concentrates on visualizing the power flow solution set on boundary of the feasible region. Load security region is the power flow solution set which do not violate the power system constraints. The solutions are obtained from tracing algorithm. Tracing algorithm includes of 2 methods. The first method is the initial guess and first prediction point determination, and the other method is continuation method.

Initial guess and first prediction point are calculated by using repeated power flow with bisection method. Continuation method consists of 2 processes. The first process is prediction process. This process is used to provide the prediction point where the first prediction point is obtained from the first method. Additionally, the prediction point is the point which is outside the feasible region. The second process is corrector process. This process is used to correct the prediction point to the power flow solution on boundary of the feasible region. The corrector process is replaced by optimization-base method. This method is used to find the shortest distance between the prediction point and the solution on the boundary. Optimization-based method is nonconvex and nonlinear problem. This thesis proposes SOCP relaxation to convexify the conventional optimization-based method to be convex problem. The process is repeated until the correction point set is a contour of the feasible region.

From the chapter 6, this research tests on six-bus, nine-bus system, and 24-bus system. This thesis sets the test into 4 conditions. First condition is power transfer from all source bus to sink bus for base case test system. Second condition is power transfer from area to area. Third condition is base case test system with load shedding. Last condition is base case test system with PV installing. All generator buses are set as source bus of all cases. In addition, source bus supplies active and reactive power to the power system. Sink bus is set upon each condition and consumes the power from the power system. This thesis considers the load demand on sink bus which is related to source bus. This load security region is visualized on P-Q plane and used to describe the maximum active and reactive load demand in every direction. System parameter, which is load shedding and photovoltaic (PV) installing, affects to the load security region shape. From load shedding, the load security region can be expanded because of reducing another load demand and can be moved because total load demand must larger than minimum generator limit. From PV installation, the load security region of PV installed bus is expanded as PV size. On the other hand, the total generation capacity is increased so load security region is also increased up to power system limit. Finally, the load security region presents the robustness of the power system by the load demand expansion without the violation.

7.2 Future Work

This work develops the tracing algorithm with SOCP relaxation to visualize the load security of the power system. However, this research only considers the small-scale power system which is not complicated system. Besides, the test system is a base case system. Thereby, the future work can apply this tracing algorithm to other problems, such as, the larger-scale power system problem, the complicated power system which is more than one generator in one bus or has specific constraint. Likewise, the additional devices are also applied to the power system, for instance, solar cell in other propose, static var compensator (SVC), and others. Last but not least, the load security region data can be used to plan, design, or schedule the power system, such

as, load expansion. Ultimately, the computation time can be improved to obtain the load security region faster than this method by using other processes instead of continuation method.

REFERENCES

REFERENCES

[1]   H. Marefatjou, and I. Soltani, "Continuation Power Flow Method with Improved Voltage Stability Analysis in Two Area Power System" International Journal of Electrical Energy, vol. 1, no. 1, 2013.

[2]   P. W. Pande, S. Kumar and A. K. Sinha, "Total Transfer Capability calculation using Modified Repeated Power flow Method," 2015 Annual IEEE India Conference (INDICON), New Delhi, India, 2015, pp. 1-6.

[3]   I. A. Hiskens and R. J. Davy, "Exploring the power flow solution space boundary," in IEEE Transactions on Power Systems, vol. 16, no. 3, pp. 389-395, Aug. 2001.

[4]   S. Limpatthamapanee, "Load feasible region determination using boundary tracing method," Ph.D., Electrical Engineering, Chulalongkorn University, 2011.

[5]   Y. Chen, J. Xiang, and Y. Li, "SOCP Relaxations of Optimal Power Flow Problem Considering Current Margins in Radial Networks," Energies, vol. 11, pp. 1-17, Nov. 2018.

[6]   T. J. Overbye, "A power flow measure for unsolvable cases," in IEEE Transactions on Power Systems, vol. 9, no. 3, pp. 1359-1365, Aug. 1994.

[7]   S. Ikeda, A. Takeda and H. Ohmori, "Optimal sizing of photovoltaic systems for loss minimization in distribution network," 2018 SICE International Symposium on Control Systems (SICE ISCS), Tokyo, Japan, 2018, pp. 185-192.

[8]   X. Zhang et al., "Optimal allocation of static var compensator via mixed integer conic programming," 2017 IEEE Power & Energy Society General Meeting, Chicago, IL, USA, 2017, pp. 1-5.

[9]   K. Lehmann, A. Grastien, and P. V. Hentenryck, "AC-feasibility on tree networks is NP-hard," *IEEE Trans. Power Syst.*, vol. 31, no. 1, pp. 798–801, Jan. 2016.

[10]   B. Stott, J. Jardim, and O. Alsac, "DC power flow revisited," IEEE Trans Power Syst., vol. 24, no. 3, pp. 1290–1300, Aug. 2009.

[11]   M. E. Baran and F. F. Wu, "Optimal capacitor placement on radial distribution systems," IEEE Trans. Power Del., vol. 4, no. 1, pp. 725–734, Jan. 1989.

[12]   M. E. Baran and F. F.Wu, "Optimal sizing of capacitors placed on a radial distribution system," IEEE Trans. Power Del., vol. 4, no. 1, pp. 735–743, Jan. 1989.

[13]   R. A. Jabr, "A primal-dual interior-point method to solve the optimal power flow dispatching problem," Optim. Eng., vol. 4, pp. 309–336, 2003.

[14]   W. Min and L. Shengsong, "A trust region interior point algorithm for optimal power flow problems," Int. J. Elect. Power Energy Syst., vol. 2, pp. 293–300, 2005.

[15]   E. C. Baptista, E. A. Belati, and G. R. M. da Costa, "Logarithmic barrier augmented lagrangian function to the optimal power flow problem," Int. J. Elect. Power Energy Syst., vol. 27, pp. 528–532, 2005.

[16]   A. G. Bakirtzis, P. N. Biskas, C. E. Zoumas, and V. Petridis, "Optimal power flow by enhanced genetic algorithm," IEEE Trans. Power Syst., vol. 17, no. 2, pp. 229–236, May 2002.

[17]   M. A. Abido, "Optimal power flow using particle swarm optimization," Int. J. Elect. Power Energy Syst., vol. 24, pp. 563–571, Sep. 2002.

[18]   . Coffrin and P. Van Hentenryck, "A linear-programming approximation of AC power flows," INFORMS J. Comput., vol. 26, pp. 718–734, 2014.

[19]   J. Lavaei and S.H. Low, "Zero duality gap in optimal power flowproblem," IEEE Trans. Power Syst., vol. 27, no. 1, pp. 92–107, Feb. 2012.

[20]   D. K. Molzahn and I. A. Hiskens, "Moment-based relaxation of the optimal power flow problem," in Proc. Power Syst. Comput. Conf., 2014, pp. 1–7.

[21]   D. K. Molzahn and I. A. Hiskens, "Sparsity-exploiting moment-based relaxations of the optimal power flow problem," IEEE Trans. Power syst., vol. 30, no. 6, pp. 3168–3180, Nov. 2015.

[22]   E. Dall'Anese, G. B. Giannakis, and B. F. Wollenberg, "Optimization of unbalanced power distribution networks via semidefinite relaxation," in Proc. 2012 North Amer. Power Symp., Champaign, IL, USA, 2012, pp. 1–6.

[23]   L. Gan and S. H. Low, "Convex relaxations and linear approximation for optimal power flow in multiphase radial networks," in Proc. 2014 Power Syst. Comput. Conf., Wroclaw, Poland, 2014, pp. 1–9.

[24]   S. Sojoudi and J. Lavaei, "Convexification of optimal power flow problem by means of phase shifters," in Proc. IEEE Int. Conf. Smart Grid Commun.,2013, pp. 756–761.

[25]   J. Lavaei, D. Tse, and B. Zhang, "Geometry of power flows and optimization in distribution networks," IEEE Trans. Power Syst., vol. 29, no. 2, pp. 572–583, Mar. 2014.

[26]   M. Farivar, C. R. Clarkey, S. H. Low, and K. M. Chandy, "Inverter VAR control for distribution systems with renewables," in Proc. 2011 Int. Conf. Smart Grid Commun., pp. 457–462, 2011.

[27]   L. Gan, N. Li, U. Topcu, and S. Low, "On the exactness of convex relaxation for optimal power flow in tree networks," in Proc. 2012 IEEE Annu. Conf. Decision Control, pp. 465–471, 2012.

[28]   G. Lingwen, L. Na, U. Topcu, and S. Low, "Exact convex relaxation of optimal power flow in radial networks," IEEE Trans. Automat. Control,vol. 60, no. 1, pp. 72–87, Jan. 2015.

[29]   R. A. Jabr, "Radial distribution load flow using conic programming," in IEEE Transactions on Power Systems, vol. 21, no. 3, pp. 1458-1459, Aug. 2006.

[30]   M. Nick, R. Cherkaoui, J. L. Boudec and M. Paolone, "An Exact Convex Formulation of the Optimal Power Flow in Radial Distribution Networks Including Transverse Components," in IEEE Transactions on Automatic Control, vol. 63, no. 3, pp. 682-697, March 2018.

[31] S. Chen, Z. Wei, G. Sun, K. W. Cheung and D. Wang, "Identifying Optimal Energy Flow Solvability in Electricity-Gas Integrated Energy Systems," in IEEE Transactions on Sustainable Energy, vol. 8, no. 2, pp. 846-854, April 2017.

[32] S. P. Boyd and L. Vandenberghe, Convex Optimization, Cambridge, U.K. Cambridge Univ. Press, 2004.

[33] M. Lobo, L. Vandenberghe, S. Boyd, and H. Lebret, "Applications of second-order cone programming," Linear Algebra and Its Applications, pp.193-284, 1998.

[34] Allen. J. Wood and Bruce F., Power Generation, Operation, and Control, 2nd Edition, 2nd ed. New York, NY, USA: John Wiley & Sons, 1996.

[35] R.P. Schulz, A.E. Turner and D.N. Ewart, "Long Term Power System Dynamics," EPRI Report 90-7-0, Palo Alto, California, 1974.

[36] สุรชัย ชัยทัศนีย์, พลังงานหมุนเวียนและการผลิตไฟฟ้าแบบกระจายตัว, กรุงเทพฯ, สำนักพิมพ์จุฬาลงกรณ์มหาวิทยาลัย, 2557.

[37] IEEE Reliability Test System Task Force of Applications of Probability Methods Subcommittee, "IEEE reliability test system-96," IEEE Transactions on Power Systems, Vol. 14, No. 3, pp. 1010-1020, Aug. 1999.

APPENDIX

APPENDIX

A. Data of Test Systems

A.1 6-Bus Test System

The 6-bus test system comprises of 3 generators, 3 load buses, and 11 branches. Bus type 1 is defined as load bus. Bus type 2 is defined as voltage bus. Bus type 3 is defined as slack bus. The data of the system is shown in Table A.1-A.3 where the system complex power base is 100 MVA.

Figure A.1 6-bus network system

Table A.1 Bus data of 6-bus test system

Bus	Bus type	P_d (MW)	Q_d (MVAr)	Area	$|V|$ (p.u.)	θ (deg.)	V_{base} (kV)	V_{max} (p.u.)	V_{min} (p.u.)
1	3	0	0	1	1.05	0	230	1.05	1.05
2	2	0	0	1	1.05	0	230	1.05	1.05
3	2	0	0	1	1.07	0	230	1.07	1.07

Bus	Bus type	P_d (MW)	Q_d (MVAr)	Area	$\|V\|$ (p.u.)	θ (deg.)	V_{base} (kV)	V_{max} (p.u.)	V_{min} (p.u.)
4	1	70	70	1	1.00	0	230	1.05	0.95
5	1	70	70	1	1.00	0	230	1.05	0.95
6	1	70	70	1	1.00	0	230	1.05	0.95

Table A.2 Generator data of 6-bus test system

Bus	P_g (MW)	Q_g (MVAr)	Q_{max} (MVAr)	Q_{min} (MVAr)	V_g (p.u.)	P_{max} (MW)	P_{min} (MW)
1	72.30	27.03	300	-300	1.040	250	10
2	163.00	6.54	300	-300	1.025	300	10
3	85.00	-10.95	300	-300	1.025	270	10

Table A.3 Branch data of 6-bus test system

Branch	From bus	To bus	R (p.u.)	X (p.u.)	B_c (p.u.)	Line limit (MVA)
1	1	2	0.10	0.20	0.04	40
2	1	4	0.05	0.20	0.04	60
3	1	5	0.08	0.30	0.06	40
4	2	3	0.05	0.25	0.06	40
5	2	4	0.05	0.10	0.02	60
6	2	5	0.10	0.30	0.04	30
7	2	6	0.07	0.20	0.05	90
8	3	5	0.12	0.26	0.05	70
9	3	6	0.02	0.10	0.02	80
10	4	5	0.20	0.40	0.08	20
11	5	6	0.10	0.30	0.06	40

A.2 9-Bus Test System

The 9-bus test system comprises of 3 generators, 6 load buses, and 11 branches. Bus type 1 is defined as load bus. Bus type 2 is defined as voltage bus. Bus type 3 is defined as slack bus. The data of the system is shown in Table A.4-A.6 where the system complex power base is 100 MVA.
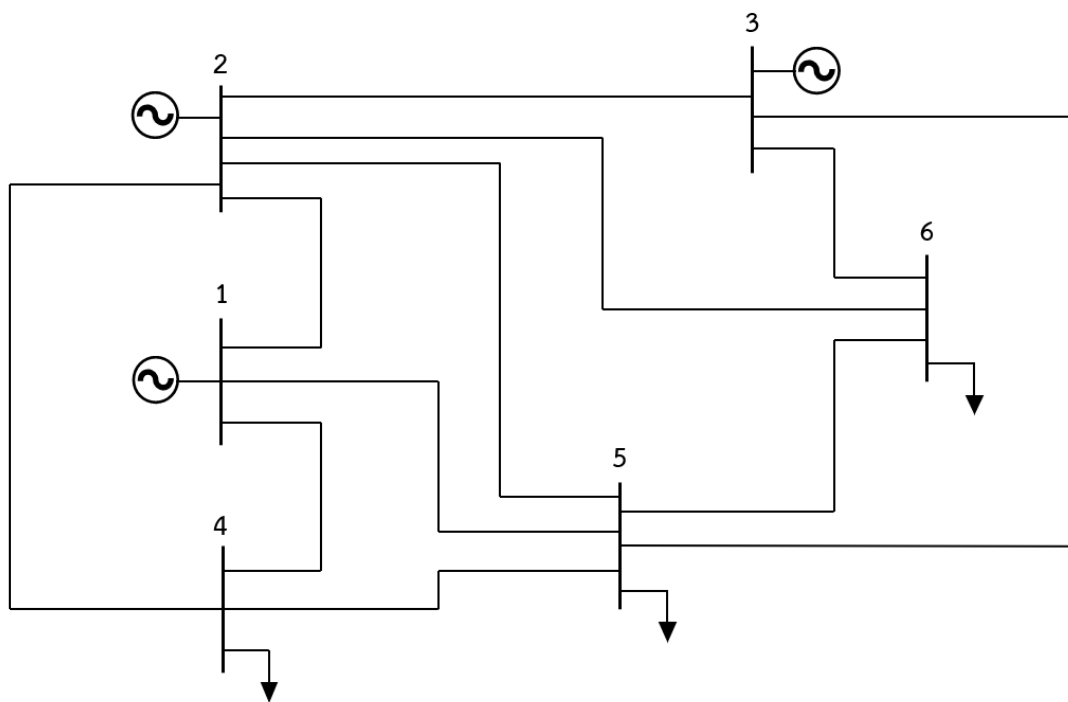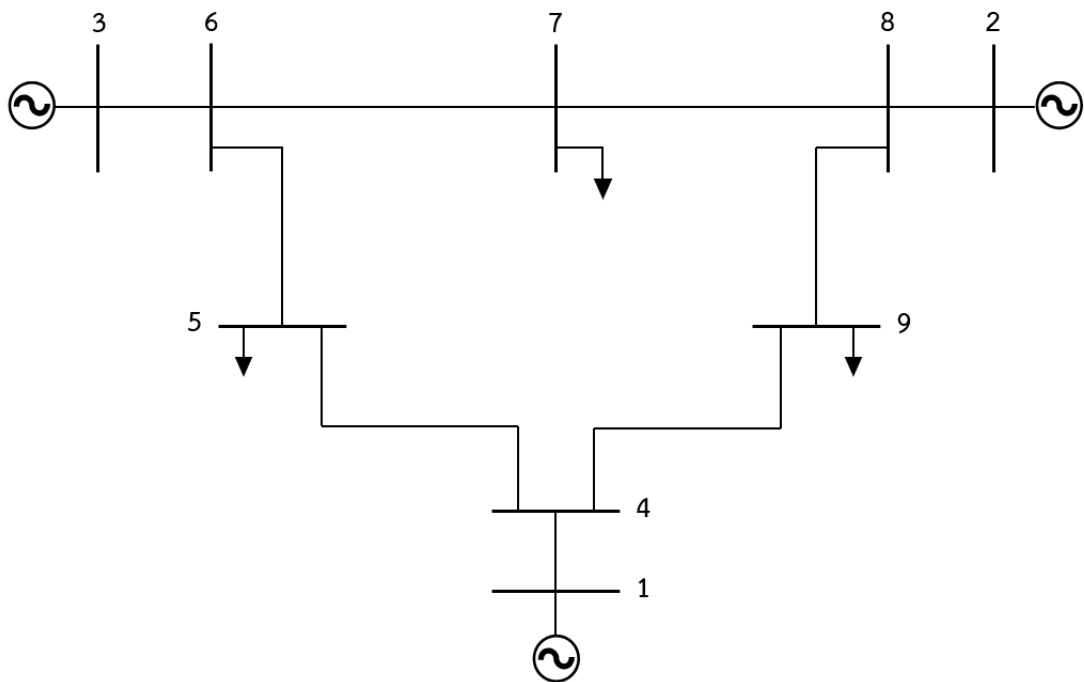

Figure A.2 9-bus network system

Table A.4 Bus data of 9-bus test system

Bus	Bus type	P_d (MW)	Q_d (MVAr)	Area	$|V|$ (p.u.)	θ (deg.)	V_{base} (kV)	V_{max} (p.u.)	V_{min} (p.u.)
1	3	0	0	1	1	0	345	1.1	0.9
2	2	0	0	1	1	0	345	1.1	0.9
3	2	0	0	1	1	0	345	1.1	0.9
4	1	0	0	1	1	0	345	1.1	0.9
5	1	90	30	1	1	0	345	1.1	0.9
6	1	0	0	1	1	0	345	1.1	0.9

Bus	Bus type	P_d (MW)	Q_d (MVAr)	Area	$\lvert V \rvert$ (p.u.)	θ (deg.)	V_{base} (kV)	V_{max} (p.u.)	V_{min} (p.u.)
7	1	100	35	1	1	0	345	1.1	0.9
8	1	0	0	1	1	0	345	1.1	0.9
9	1	125	50	1	1	0	345	1.1	0.9

Table A.5 Generator data of 9-bus test system

Bus	P_g (MW)	Q_g (MVAr)	Q_{max} (MVAr)	Q_{min} (MVAr)	V_g (p.u.)	P_{max} (MW)	P_{min} (MW)
1	72.30	27.03	300	-300	1.040	250	10
2	163.00	6.54	300	-300	1.025	300	10
3	85.00	-10.95	300	-300	1.025	270	10

Table A.6 Branch data of 9-bus test system

Branch	From bus	To bus	R (p.u.)	X (p.u.)	B_c (p.u.)	Line limit (MVA)
1	1	4	0	0.0576	0	250
2	4	5	0.017	0.092	0.158	250
3	5	6	0.039	0.17	0.358	150
4	3	6	0	0.0586	0	300
5	6	7	0.0119	0.1008	0.209	150
6	7	8	0.0085	0.072	0.149	250
7	8	2	0	0.0625	0	250
8	8	9	0.032	0.161	0.306	250
9	9	4	0.01	0.085	0.176	250

A.3 24-Bus Test System

The test system consists of 33 generators, 17 load buses, and 38 branches. The system is divided into 4 area. The information of the system is shown in Table A.7-A.9 where the system complex power base is 100 MVA.
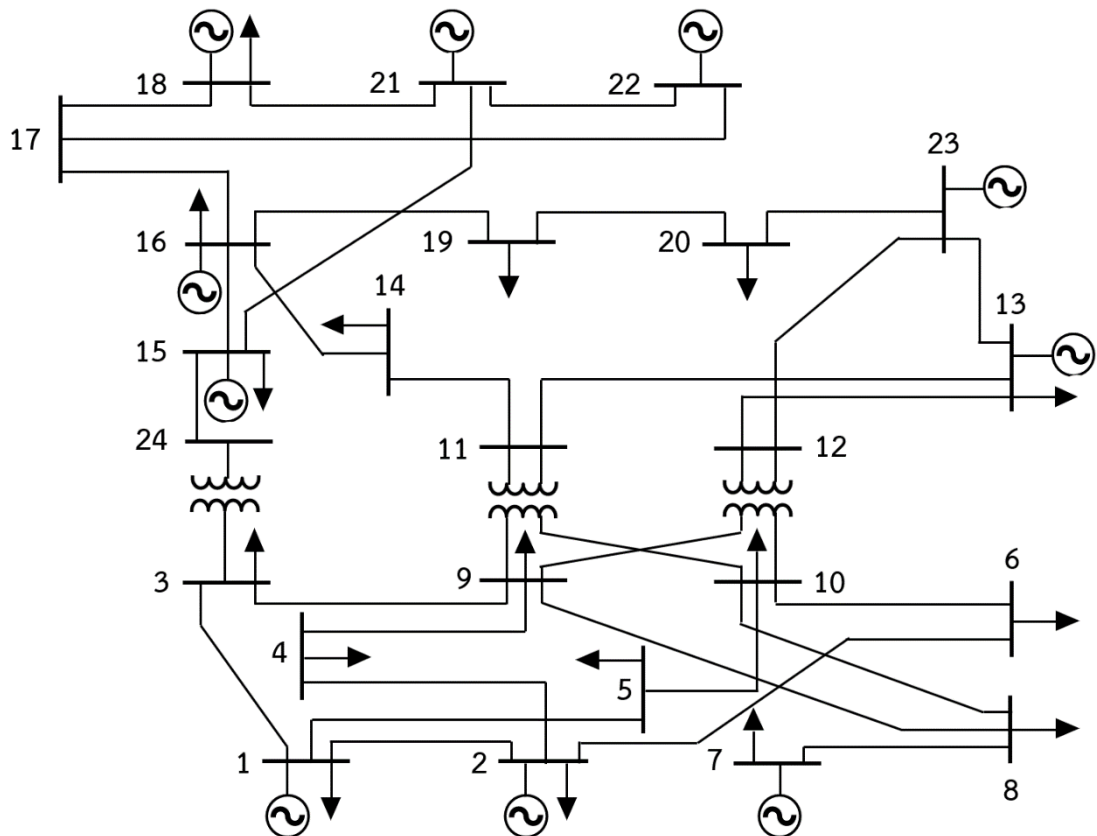

Figure A.3 24-bus network system

Table A.7 Bus data of 24-bus test system

Bus	Bus type	P_d (MW)	Q_d (MVAr)	Area	$|V|$ (p.u.)	θ (deg.)	V_{base} (kV)	V_{max} (p.u.)	V_{min} (p.u.)
1	2	108	22	1	1	0	138	1.05	0.95
2	2	97	20	1	1	0	138	1.05	0.95
3	1	180	37	1	1	0	138	1.05	0.95
4	1	74	15	1	1	0	138	1.05	0.95
5	1	71	14	1	1	0	138	1.05	0.95

Bus	Bus type	P_d (MW)	Q_d (MVAr)	Area	$|V|$ (p.u.)	θ (deg.)	V_{base} (kV)	V_{max} (p.u.)	V_{min} (p.u.)
6	1	136	28	2	1	0	138	1.05	0.95
7	2	125	25	2	1	0	138	1.05	0.95
8	1	171	35	2	1	0	138	1.05	0.95
9	1	175	36	1	1	0	138	1.05	0.95
10	1	195	40	2	1	0	138	1.05	0.95
11	1	0	0	3	1	0	230	1.05	0.95
12	1	0	0	3	1	0	230	1.05	0.95
13	3	265	54	3	1	0	230	1.05	0.95
14	2	194	39	3	1	0	230	1.05	0.95
15	2	317	64	4	1	0	230	1.05	0.95
16	2	100	20	4	1	0	230	1.05	0.95
17	1	0	0	4	1	0	230	1.05	0.95
18	2	333	68	4	1	0	230	1.05	0.95
19	1	181	37	3	1	0	230	1.05	0.95
20	1	128	26	3	1	0	230	1.05	0.95
21	2	0	0	4	1	0	230	1.05	0.95
22	2	0	0	4	1	0	230	1.05	0.95
23	2	0	0	3	1	0	230	1.05	0.95
24	1	0	0	4	1	0	230	1.05	0.95

Table A.8 Generator data of 24-bus test system

Bus	P_g (MW)	Q_g (MVAr)	Q_{max} (MVAr)	Q_{min} (MVAr)	V_g (p.u.)	P_{max} (MW)	P_{min} (MW)
1	10.0	0	10	0	1.035	20.0	16.0
1	10.0	0	10	0	1.035	20.0	16.0
1	76.0	0	30	-25	1.035	76.0	15.2
1	76.0	0	30	-25	1.035	76.0	15.2
2	10.0	0	10	0	1.035	20.0	16.0

Bus	P_g (MW)	Q_g (MVAr)	Q_{max} (MVAr)	Q_{min} (MVAr)	V_g (p.u.)	P_{max} (MW)	P_{min} (MW)
2	10.0	0	10	0	1.035	20.0	16.0
2	76.0	0	30	-25	1.035	76.0	15.2
2	76.0	0	30	-25	1.035	76.0	15.2
7	80.0	0	60	0	1.025	100.0	25.0
7	80.0	0	60	0	1.025	100.0	25.0
7	80.0	0	60	0	1.025	100.0	25.0
13	95.1	0	80	0	1.020	197.0	69.0
13	95.1	0	80	0	1.020	197.0	69.0
13	95.1	0	80	0	1.020	197.0	69.0
14	0.0	35.3	200	-50	0.980	0.0	0.0
15	12.0	0	6	0	1.014	12.0	2.4
15	12.0	0	6	0	1.014	12.0	2.4
15	12.0	0	6	0	1.014	12.0	2.4
15	12.0	0	6	0	1.014	12.0	2.4
15	12.0	0	6	0	1.014	12.0	2.4
15	155.0	0	80	-50	1.014	155.0	54.3
16	155.0	0	80	-50	1.017	155.0	54.3
18	400.0	0	200	-50	1.050	400.0	100.0
21	400.0	0	200	-50	1.050	400.0	100.0
22	50.0	0	16	-10	1.050	50.0	10.0
22	50.0	0	16	-10	1.050	50.0	10.0
22	50.0	0	16	-10	1.050	50.0	10.0
22	50.0	0	16	-10	1.050	50.0	10.0
22	50.0	0	16	-10	1.050	50.0	10.0
22	50.0	0	16	-10	1.050	50.0	10.0
23	155.0	0	80	-50	1.050	155.0	54.3
23	155.0	0	80	-50	1.050	155.0	54.3
23	350.0	0	150	-25	1.050	350.0	140.0

Table A.9 Branch data of 24-bus test system

Branch	From bus	To bus	R (p.u.)	X (p.u.)	B_c (p.u.)	Line limit (MVA)
1	1	2	0.0026	0.0139	0.4611	175
2	1	3	0.0546	0.2112	0.0572	175
3	1	5	0.0218	0.0845	0.0229	175
4	2	4	0.0328	0.1267	0.0343	175
5	2	6	0.0497	0.1920	0.0520	175
6	3	9	0.0308	0.1190	0.0322	175
7	3	24	0.0023	0.0839	0.0000	400
8	4	9	0.0268	0.1037	0.0281	175
9	5	10	0.0228	0.0883	0.0239	175
10	6	10	0.0139	0.0605	2.4590	175
11	7	8	0.0159	0.0614	0.0166	175
12	8	9	0.0427	0.1651	0.0447	175
13	8	10	0.0427	0.1651	0.0447	175
14	9	11	0.0023	0.0839	0.0000	400
15	9	12	0.0023	0.0839	0.0000	400
16	10	11	0.0023	0.0839	0.0000	400
17	10	12	0.0023	0.0839	0.0000	400
18	11	13	0.0061	0.0476	0.0999	500
19	11	14	0.0054	0.0418	0.0879	500
20	12	13	0.0061	0.0476	0.0999	500
21	12	23	0.0124	0.0966	0.2030	500
22	13	23	0.0111	0.0865	0.1818	500
23	14	16	0.005	0.0389	0.0818	500
24	15	16	0.0022	0.0173	0.0364	500
25	15	21	0.0063	0.0490	0.1030	500
26	15	21	0.0063	0.0490	0.1030	500

Branch	From bus	To bus	R (p.u.)	X (p.u.)	B_c (p.u.)	Line limit (MVA)
27	15	24	0.0067	0.0519	0.1091	500
28	16	17	0.0033	0.0259	0.0545	500
29	16	19	0.003	0.0231	0.0485	500
30	17	18	0.0018	0.0144	0.0303	500
31	17	22	0.0135	0.1053	0.2212	500
32	18	21	0.0033	0.0259	0.0545	500
33	18	21	0.0033	0.0259	0.0545	500
34	19	20	0.0051	0.0396	0.0833	500
35	19	20	0.0051	0.0396	0.0833	500
36	20	23	0.0028	0.0216	0.0455	500
37	20	23	0.0028	0.0216	0.0455	500
38	21	22	0.0087	0.0678	0.1424	500

NAME	Pongsakorn Sukheeboon
DATE OF BIRTH	22 August 1996
PLACE OF BIRTH	Bangkok, Thailand
INSTITUTIONS ATTENDED	B. Eng. (Electrical Eng.) at Chulalongkorn University
	M. Eng. (Electrical Eng.) at Chulalongkorn University
HOME ADDRESS	Power System Research Lab (PSRL) 12th floor, Building 4, Department of Electrical Engineering, Faulty of Engineering, Chulalongkorn University

จุฬาลงกรณ์มหาวิทยาลัย

CHULALONGKORN UNIVERSITY